NOx CONCENTRATION MEASUREMENT IN AMBIENT AIR OF DHAHRAN

BY

MUMIN ABDULAHI

A Thesis Presented to the
DEANSHIP OF GRADUATE STUDIES

KING FAHD UNIVERSITY OF PETROLEUM & MINERALS

DHAHRAN, SAUDI ARABIA

In Partial Fulfillment of the
Requirements for the Degree of

MASTER OF SCIENCE

In

PHYSICS

APRIL, 2016

KING FAHD UNIVERSITY OF PETROLEUM & MINERALS

DHAHRAN 31261, SAUDI ARABIA

DEANSHIP OF GRADUATE STUDIES

This thesis, written by **MUMIN ABDULAHI** under the direction of his thesis advisor and approved by his thesis committee, has been presented to and accepted by Dean of Graduate Studies, in partial fulfillment of the requirements for the degree of **MASTER OF SCIENCE IN PHYSICS.**

Dr. Khaled Gasmi
(Advisor)

Dr. Abdul-Aziz Al-Jalal (Member)

Prof. Fida F. Al-Aldel (Member)

Dr. Abdullah A. Al-Sunaidi
Chairman, Department of Physics

Dr. Salam A. Zummo
Dean of Graduate Studies

8/5/16
[Date]

This thesis is dedicated to my family

ACKNOWLEGEMENTS

This research was funded by King Abdulaziz City for Science and Technology (KACST) through the Science and Technology Unit at King Fahd University of Petroleum and Minerals (KFUPM) with the project number, 12-ENV2365-04 as part of National Science, Technology and Innovation Plan.

I really appreciate the effort of my supervisor, Dr. Khaled Gasmi, who has contributed immensely to the success of this work. His patience and endurance with me as a student of learning is quite unprecedented. Never was it a time I needed his attention that he did not respond positively. He is more than an ordinary teacher but an epitome of a good emulator and pacesetter; you are really appreciated sir.

This acknowledgement would not have been complete without recognizing the contribution to this work through my committee member, in the person of Dr Abdul–Aziz Al-Jalal whose academic distinction and scientific understanding had a great deal of positive impact on the outcome of this thesis. To this end I say to him, big thanks for his both financial and academic support. The positive contribution of Prof. Fida F. Al-Aldel who is as well a committee member cannot also be overemphasized as he made positive remarks which added to this thesis report, a good scent of scientific touch. Also I will not fail to recognize the optic lab research members in the persons of Dr. Watheq Ahmed Al-Basheer, for his sweet words of encouragement and Mr. Taofeek Adigun for the mutual support.

The efforts of my parents, Mr. Abdulahi Abdul-Salam and Mrs. Sidikat Abdulahi, to raise me up as a good child are really appreciated, in fact they are the source of my strength and energy, nothing would I have been able to achieve without them; thank you for being good parents to me. More so, I really recognize and appreciate my lovely wife, Mrs Muslimah Olaitan Abdulahi nee Folarin, whose perseverance and sacrifice through the journey of this study, is second to none. She waited patiently for me in my country while I was away for the academic pursuit, nothing of beautiful words or monetary reward could match what you have done, just accept this sincere appreciation from me. My siblings in the person of Mrs Kafayat, Mrs Nafisat and Mr. Yaquub are also remembered for their prayers over me, while I never forget to pray for my late sister, Mrs. Suliyat who recently returned to her creator for peaceful repose of her soul, I really miss her so much.

I really appreciate my well-wishers and friends both in Nigeria and KFUPM who have contributed in one way or the others to my academic success; they will continue to live forever in my mind.

Table of Contents

LIST OF FIGURES

LIST OF TABLES

LIST OF ABREVIATIONS

g	:	Acceleration due to Gravity
M	:	Air Mass
AM	:	Ante Meridian
CO	:	Carbon monoxide
CRDS	:	Cavity Ring Down Spectroscopy
R^2	:	Coefficient of Determination
Coef	:	Coefficient
C/ Conc.	:	Concentration
V	:	Controlled Air Volume
Q	:	Daily Fuel Consumption
DOAS	:	Differential Optical Absorption Spectroscopy
K	:	Emission Factor
F_B	:	Emissive Power
EU	:	European Union
R	:	Gas Constant
H	:	Heat Transfer
InHg	:	Inch of Mercury
LIF	:	Laser Induced Fluorescence
LT	:	Local Time
MPH	:	Mile Per Hour
NO2	:	Nitrogen dioxide
NO	:	Nitrous oxide
NOx	:	Nitrogen oxides
N_2	:	Nitrogen Gas
NAAQS	:	National Ambient Air Quality Standards National Ambient Air Quality Standards
O_3	:	Ozone

O_2	:	Oxygen Molecule
Ppb	:	Part Per Billion
Ppm	:	Part Per Million
PC	:	Personal Computer
PMT	:	Photomultiplier Tube
υ	:	Photon frequency
h	:	Planck's Constant
P/Pres	:	Pressure
PM	:	Post Meridian
H/ RH	:	Relative Humidity
J	:	Rate of NO_2 photolysis
k	:	Rate coefficient for $NO + O_3$
REMPI	:	Resonance Enhanced MultiPhoton Ionisation
SO_2	:	Sulphur dioxide
σ	:	Stefan Constant
SE	:	Standard Error
T	:	Temperature
TDLAS	:	Tunable Diode Laser Absorption Spectroscopy
t_f	:	Transit time in forward Direction
t_r	:	Transit Time in Reverse Direction
U	:	Total Heat Transfer Coefficient
USEPA	:	United State Environmental Protection Agency
V_w/ S	:	Wind Speed
WHO	:	World Health Organization

ABSTRACT

Full Name : Mumin Abdulahi

Thesis Title : NOx Concentration Measurement in Ambient Air of Dhahran

Major Physics : Physics

Date of Degree : April, 2016

NOx ($NO + NO_2$) concentration and meteorological parameters (temperature, pressure, relative humidity, wind speed and wind direction) measurement were carried out in Dhahran between 8^{th} of May, 2015 and 30^{th} of July 2015 using chemiluminesce-based NOx analyser and weather station respectively. Hourly mean and daily average of the real time acquired data were computed using Mathematica program for the purpose of studying daily and hourly variation of NOx with weather parameters. Temperature and wind speed showed their peak value in the afternoon. While ambient air pressure was nearly constant throughout the period, relative humidity reached its peak value in the night and early morning. NO_2 average concentration of 41.2 ppb was measured, which is lower than USEPA exposure limit. However, there were eighteen occurrences where 100 ppb permissible limit by USEPA was exceeded. NOx concentration in Dhahran was largely being influenced by traffic emission. In addition to this, photochemical reaction and weather condition also affect the NOx episode in the city. Regression analysis of the daily hourly mean of the data showed that temperature and wind speed show negative correlation coefficients while relative humidity shows positive correlation coefficient with NOx concentration. Semi empirical model, with R^2 greater than 0.5, was formulated using the NOx and meteorological data acquired.

ملخص الرسالة

تم قياس أكاسيد النيتروجين ($NO + NO_2$) التركيز ومتغيرات الأرصاد الجوية (درجة الحرارة والضغط والرطوبة النسبية وسرعة الرياح واتجاه الرياح) في الظهران بين 8 مايو 2015 و30 يوليو 2015 باستخدام التوهج من أكاسيد النيتروجين محلل ومحطة الطقس على التوالي. تم حساب البيانات التي تم جمعها في الوقت الحقيقي مع البرامج الحاسوبية الرياضيات لغرض دراسة التغيرات اليومية وأيضا اختلافات كل 60 دقيقة أكاسيد النيتروجين مع متغيرات الطقس. وأظهرت قياسات درجة الحرارة وسرعة الرياح قيمة الذروة في فترة ما بعد الظهر. وكانت قياسات ضغط الهواء المحيط ثابتة تقريبا خلال هذه الفترة، وصلت الرطوبة النسبية قيمة ذروتها في ساعات الليل والصباح الباكر. تم حساب متوسط تركيزات NO_2 من 41.2 جزء في البليون، وهو أقل من حد التعرض من قبل وكالة حماية البيئة المحددة في الولايات المتحدة الأمريكية.بالرغم من أن هنالك 18 حالات حدوث في كل ساعة فالحد الأدني المسموح هو 100 جزء من البليون قد تم تجاوزها. وخلص إلى أن تركيز أكاسيد النيتروجين في الظهران كان إلى حد كبير أن تتأثر انبعاث حركة المرور. بالإضافة إلى ذلك، فإن تفاعل كيميائي ضوئي، وحالة الطقس تؤثر أيضا على الحلقة أكاسيد النيتروجين في المدينة. وأظهر تحليل الانحدار للمتوسط بالساعة اليومي للبيانات أن درجة الحرارة وسرعة الرياح ومعاملات علاقة عكسية بينما أظهرت الرطوبة النسبية معامل ارتباط إيجابي مع تركيز أكاسيد النيتروجين. وقد وضعت نموذج تجريبي بسيط من R^2 أكبر من 0.5 باستخدام تركيزات أكاسيد النيتروجين وبيانات الأرصاد الجوية التي تم الحصول عليها

CHAPTER 1

1.0 INTRODUCTION

1.1 Overview

The measurement of concentrations of photochemical oxidants most especially harmful ones in the ambient air is definitely imperative in the present days of industrialized world, as they have been described as being main agents affecting air quality in urban areas, and especially in the cities undergoing very fast industrial and urban expansion[1]–[3]. Furthermore, air pollution is a severe problem throughout the world as it hampers sustainable development and growth [4]. These episodes of air pollution in major urban cities are not unconnected with human activities. Unabated combustion of fossil fuels in the last century is responsible for the progressive alteration in the atmospheric composition [5]. This is so because air pollutants, such as carbon monoxide (CO), sulphur dioxide (SO_2), nitrogen oxides (NO_x), volatile organic compounds (VOCs,) ozone (O_3), heavy metals, and respiratory particulate matter ($PM_{2.5}$ and PM_{10}), which are all mostly products of human activities, differ in their chemical compositions, reaction properties, emission, time of disintegration and ability to diffuse in long or short distance [6].

Nitrogen Oxides ($NOx = NO + NO_2$), which are the subjects of this research, are one of the major pollutants, which may further lead to the formation of other harmful pollutants such as ozone, acid rain, and photochemical smog through photochemical reactions [5]. In addition, they may react with other compounds available in the atmosphere to form small particles that can be harmful to human health [6]. For example, in Saudi Arabia,

NO_2 has been found to have, to some extent, a certain positive correlation with a number of cancer cases [7]. The low levels of nitrogen oxide in the air can irritate eyes, nose, throat, and lungs, possibly causing cough and shortness of breath, tiredness and nausea. Exposure to low levels can also result in fluid build-up in the lungs within 1 or 2 days after exposure. Breathing high levels of nitrogen oxides can cause rapid burning, spasm, and swelling of tissues in the throat and upper respiratory tract in lungs, and finally death [8].

The issue with the nitrogen oxides has been dated back to early twentieth century. The widespread use of automobiles and the increase in industrial activities led to the prevalence of this type of air pollution referred to then as photochemical smog. It was most noticeable and formed almost daily in Los Angeles, California and its constituent was not elucidated until 1951 when Arie Haagen –Smit produced ozone in a laboratory from oxides of nitrogen and reactive organic gases, in the presence of sunlight and suggested that these gases were the main constituents of Los Angeles air pollution [9]. Ever since then, photochemical smog has been observed in most cities.

Although significant amount of nitrogen oxides is produced naturally, for example, during lightning and from microbial activities in soils, the main source of NO_x production in urban and industrial areas is from fossil fuel combustions, in particular, emission from car engines[10]–[13]. In addition, NO_x are very reactive and plays a significant role in the chemistry of the atmosphere and their concentration varies significantly over the course of the day with a typical residence time of about few days [14]. Inventory of NO_x emission can be quite uncertain because, while natural sources of NO_x are inherently difficult to measure, emission factor of anthropogenic sources strongly depends on the

fuel type, technology and combustion condition which makes it somewhat not easy to ascertain [10].

Nitrogen oxides are a mixture of gases that are composed of nitrogen and oxygen. Two of the most toxicologically significant nitrogen oxides are nitric oxide and nitrogen dioxide; both are nonflammable and colorless to brown at room temperature. Nitric oxide is a sharp sweet-smelling gas at room temperature, whereas nitrogen dioxide has a strong, harsh odor and is a liquid at room temperature, becoming a reddish-brown gas above 21.1 ^{o}C [8].

As much as emission plays a significant role in air quality assessment, once pollutants are emitted into the air, the weather (air temperature, air pressure, relative humidity, wind speed and wind direction) largely determines how well they disperse. Turbulence mixes pollutants into the surrounding air. As an example, during a hot summer day, the air near the surface can be much warmer than the air above. Sometimes large volumes of this warm air will rise to great heights. This results in vigorous mixing. Sometimes the condition of the atmosphere is very still (stable) and there is very little mixing. This occurs when the air near the surface of the earth is cooler than the air above. This cooler air is heavier and will not want to move up to mix with the warmer air above. Any pollutants released near the surface will get trapped and build up in the cooler layer of air near the surface. Temperature inversions are very common especially in mountain valleys, always forming during calm clear nights with light winds. They can even persist throughout the day during the winter. Wind speed also contributes to how quickly pollutants are carried away from their original source. However, strong winds don't always disperse the pollutants. They can transport pollutants to a larger area, such as the

smoke from open burning or forest fires. Owing to this, meteorological circulation pattern has always been fingered as one of the major contributors to the dispersion and diffusion of air pollution. The interaction of emissions with meteorological circulation pattern greatly shows high correlation in air quality monitoring in many urban cities [13].

Large urban areas are often located in area with complicated and complex wind pattern probably because of their coastal location or proximity to mountain ranges. For instance, a city like Los Angeles is on the coastal region and has a close proximity to the mountain ranges with strong sunlight leading to its high episodes of intense photochemistry [15]. Three dimensional wind patterns in the basin was studied and analyzed, and it was found that the sea breeze transports the polluted air mass up the mountain slopes and as the synoptic force going weaker, a reservoir layer of these transported polluted air mass forms and then descends on the city the following morning [16]. Similar scenarios were observed in the cities like Houston [17], Phoenix [18] and a host of other cities.

Many regulatory environmental agencies around the world set safe limits for the concentration of NO_2 in ambient air. Usually two safe limits are established for this purpose one for long-term exposure averaged over one year and the second is for short-term exposure averaged over one hour. The US Environmental Protection Agency (US EPA) sets the safe limit of 53 ppb averaged over one-year and 100 ppb averaged over one hour [19]. The European Commission Department responsible for EU policy on the environment (The Directorate-General for Environment) sets even tighter limit for long-term exposure of 20 ppb averaged over one year and 100 ppb averaged over one hour not to be surpassed on more than eighteen occasions each year [20]. In 2006, the

World Health Organization (WHO) set similar safe limits for atmospheric NO_2 as US EPA.

1.2 Motivation

Dhahran is one of the major cities in Eastern province of Saudi Arabia and is the host of the largest oil company in the world, Saudi ARAMCO. Ghawar oil field, which is the largest conventional oil field in the world, is located at a distance of about 85 km from Dhahran. On the other hand, Dhahran is increasing rapidly and it is close to two big cities that are also expanding quickly, Dammam and Khobar. In addition, it is close to Jubail, the biggest industrial city in Saudi Arabia that hosts many different chemical and industrial plants. Traffic has also rapidly increased in Dhahran and its surroundings. A high number of vehicles per capita and a dense road network today characterizes Dhahran. Moreover, Saudi Arabia is one of the many arid lands in the world. Very little attention was paid to areas having the same arid environmental condition to monitor and measure actual air pollution concentration in the atmosphere. Though, monitoring of these oxidants is well established, for example, in Europe, its episode is not well understood here in Dhahran. No previously published work, to our knowledge, has ever been carried out on the analysis of NO_x as a function of meteorological data in this city, which makes it difficult to have a verifiable reference as to the level of these pollutant oxidants, and their (NO_x pollutants) behavior with meteorological data. This reason motivated the conception of this research as it will, at least, try to fill this lacuna and keep us abreast of the levels of these toxic gases in ambient air which will prompt the implementation of policy capable of averting or mitigating the damages their large presence could cause.

1.3 Objectives and Goals

The goals of this research are as follow:

- To carry out NO, NO_2 and NO_X concentration measurement in ambient air in Dhahran using chemiluminescence technique,
- To Investigate the effect of temperature, pressure, relative humidity and wind on the concentrations of NO, NO_2 and NO_X.
- To investigate the difference in NO, NO_2 and NO_X concentrations between weekdays and weekends,
- To investigate the relationship between the concentrations of NO, NO_2 and NO_X.
- To formulate a simple mathematical model to predict the NO_x concentration given meteorological data.

CHAPTER 2

2.0 BACKGROUND

2.1 Atmosphere

This is the layer of gas that envelopes the earth. It is generally believed to have formed during degassing of the Earth's interior which led to the expulsion of many volatile compounds. Physical characteristics of the atmosphere serve as the ground for describing it. The concentration of the constituents of the atmosphere decreases with the height until it levels up with the outer space emptiness. Consequently, atmosphere can be thought of as becoming extinct at a height of 500-600 km above mean sea level, though atmosphere has no definite upper boundary [21].

2.1.1 Layers of Atmosphere

From the surface of the earth upward, the atmosphere is divided into layers. In general, it is divided into lower region which is generally thought to extend to the top of stratosphere, a height of about 50 km, and upper regions, which extends from the top of stratosphere to the emptiness of the outer space. The variation in the temperature in the atmosphere with the height serves as the basis for which the earth's atmosphere is characterized. These layers are referred to as spheres and they are namely: the troposphere, the stratosphere, the mesosphere, and the thermosphere and so on. And the regions separating one layer from the other are tropopause, separating troposphere and stratosphere, stratopause, separating stratosphere and mesosphere and a host of others.

Troposphere. This is the region in the atmosphere, extending from the Earth's surface up to the tropopause, boundary between the troposphere and the next layer, which is at 10 to 15 km altitude depending on the latitude and the time of the year. This layer has the

peculiarity of decreasing temperature with height and also rapid vertical mixing (convection process).

Stratosphere. It ranges from the tropopause to the stratopause (approximately 45 to 55 km altitude). In this region temperature increases with the altitude, thereby resulting in a layer with slow vertical mixing (convention process).

Mesosphere. This region extends from the stratopause to the mesopause (approximately 80 to 90 km altitude) which is characterized with decrease in temperature with altitude up to the mesopause, a coldest region in the atmosphere. Rapid vertical mixing is also observed here.

Thermosphere. This region is above the mesopause; characterized by high temperature due to the absorption of short wavelength radiation from the Sun by nitrogen and oxygen molecules. Due to the high temperature in this region, rapid vertical mixing is observed. The ionosphere falls into this region between the upper mesosphere and lower thermosphere where plasma is formed by photoionization.

Exosphere. This is the outermost region of the atmosphere (> 500 km altitude) where gas molecules with sufficient energy can escape the Earth's gravitational potential and disappears into outer space.

This whole classification is summarily represented in figure 1.

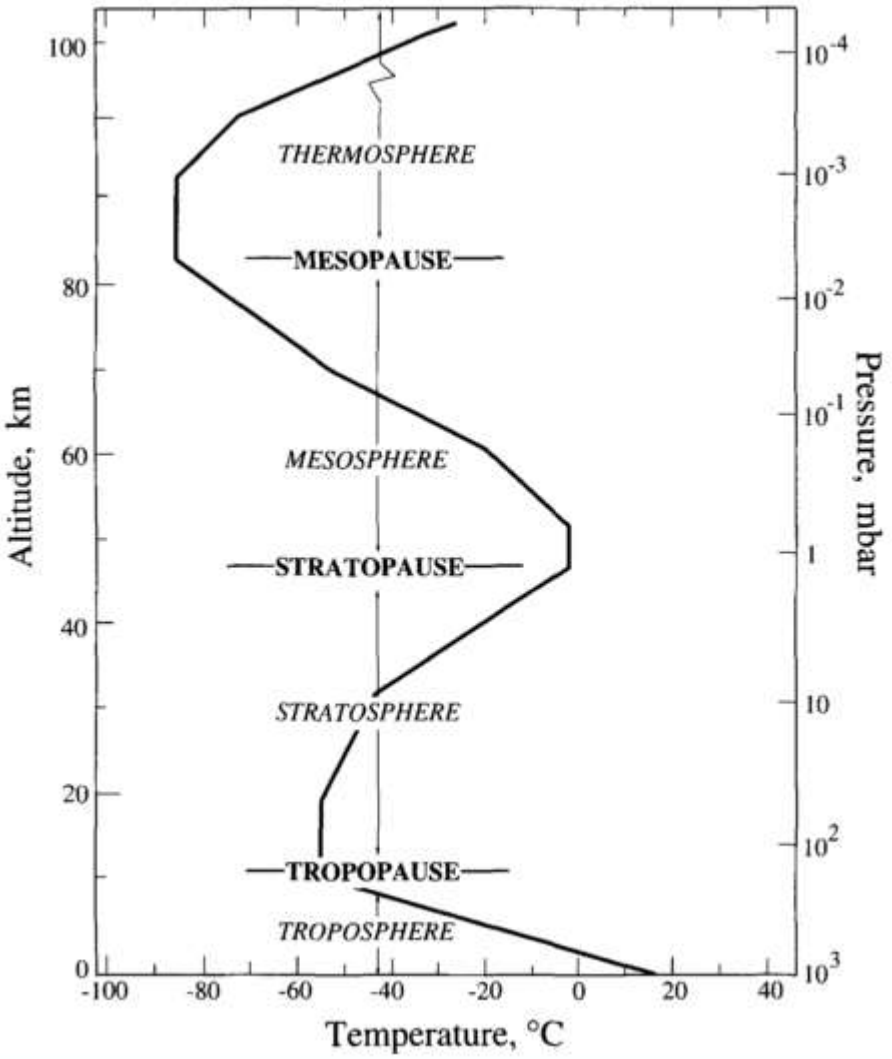

FIGURE 1: TEMPERATURE PROFILE OF ATMOSPHERE [21]

2.1.2 Composition of Atmosphere

The atmosphere is composed majorly of nitrogen, oxygen, and several noble gases whose concentrations are found considerably constant over time. In addition, there is a number of trace gases that occur in relatively small amounts.

Although atmosphere may seem unchanging in nature, it is indeed in reality a dynamic system, with its gaseous constituents continuously being swapped with the oceans, vegetation, and biological organism. The cycle of these atmospheric species involves both the physical and chemical processes which can remove or add constituents to the atmosphere.

2.1.3 Planetary Boundary Layer

This is the layer in the lowest region of troposphere known for its involvement in atmospheric pollution in urban area, the region of atmosphere governing the transport and dispersion of air pollutants, approximately the lowest 1000 m to the Earth's surface. In this layer, physical quantities including flow velocity, temperature, moisture, etc show drastic functions (turbulence) with strong vertical mixing. Physical laws and equations of motion, which dominate the planetary boundary layer dynamics and microphysics, are strictly non-linear and considerably affected by properties of Earth's surface and evolution of the process in the free atmosphere (upper troposphere). Wind structure is greatly influenced by the situation of this layer.

2.1.4 Variation of Pressure with Height in the Atmosphere

The pressure in the atmosphere varies across the layers of the atmosphere and this variation can be described by hydrostatic equation.

$$\frac{dP(z)}{dz} = -\rho(z)g \tag{2.1}$$

Where $\rho(z)$ mass air density at height z and g is acceleration due to gravity.

With the integration carried out, the pressure across the layer of atmosphere is found to be decreasing exponentially with the height as shown in the equation (2.2)

$$\frac{P(z)}{Po} = e^{-\frac{Z}{H}} \tag{2.2}$$

Where H = $\frac{RT}{Mg}$ is called the scale height

T is air temperature, M is the molar mass of air mass, g is acceleration due to gravity, H is scale height, Po is the pressure at the reference height, P (z) is the pressure at height z and R is gas constant [21].

2.1.5 Solar Radiation

All the energy reaching the earth comes from the Sun. The Earth weather is as a result of loss and absorption of radiant energy by the Earth-atmosphere system, both on global and local scale. As such, the average temperature on the Earth remains fairly constant, implying that the earth-atmosphere system loses to the space by irradiation as much as their absorbed radiation from the Sun. Therefore the accounting for the incoming and outgoing radiation energy maintains the Earth's energy balance. In balancing the Earth's energy distribution, atmosphere plays an important role by preventing some of the Sun radiation energy from getting to the surface of the earth and also controlling the amount of outgoing terrestrial radiation escaping into the outer space [22].

Apart from providing the energy to the Earth-atmosphere system and thereby ensuring the climatology where life can be feasible, solar radiation has many direct influences on the biosphere, the narrow region of the Earth- atmosphere- ocean system where living organism are flourishing. Not only that, there are indirect effects and complex feedback systems among the atmosphere, biosphere and radiative transfer, most especially when

human activities are considered as part of biosphere, for instance anthropogenic emission of CO, NO_2 and depletion of ozone layer.

2.1.6 Absorption of Radiation by Gases

The spectrum of solar radiation passes through the atmosphere is drastically altered due to the absorption by some of the gaseous constituents of the atmosphere. The most pronounced absorption of the solar and terrestrial radiation is due to not gases which are abundant in the atmosphere, N_2, O_2 but the minor constituents such as ozone, carbon dioxide, methane and water vapor. Hence, ozone in the upper atmosphere absorbs effectively all radiation below 290 nm while carbon dioxide and water vapour absorb much of radiation of the long-wavelength terrestrial radiation.

2.2 Sources of Trace Gases

Trace gases are mostly found at the troposphere; in fact the burden of trace gases is only relevant in this atmospheric layer. The main source of trace gases is emission which can be broken down into anthropogenic (man-made) and biogenic (natural emission). Example of anthropogenic source includes aircraft, burning of fossil fuel and biomass, application of fertilizer while lightening, nitrogen cycle, and etcetera form the biogenic source of this pollutant. The summary of percentage distribution of nitrogen oxides emission source (global inventory) is concisely presented in figure 2.

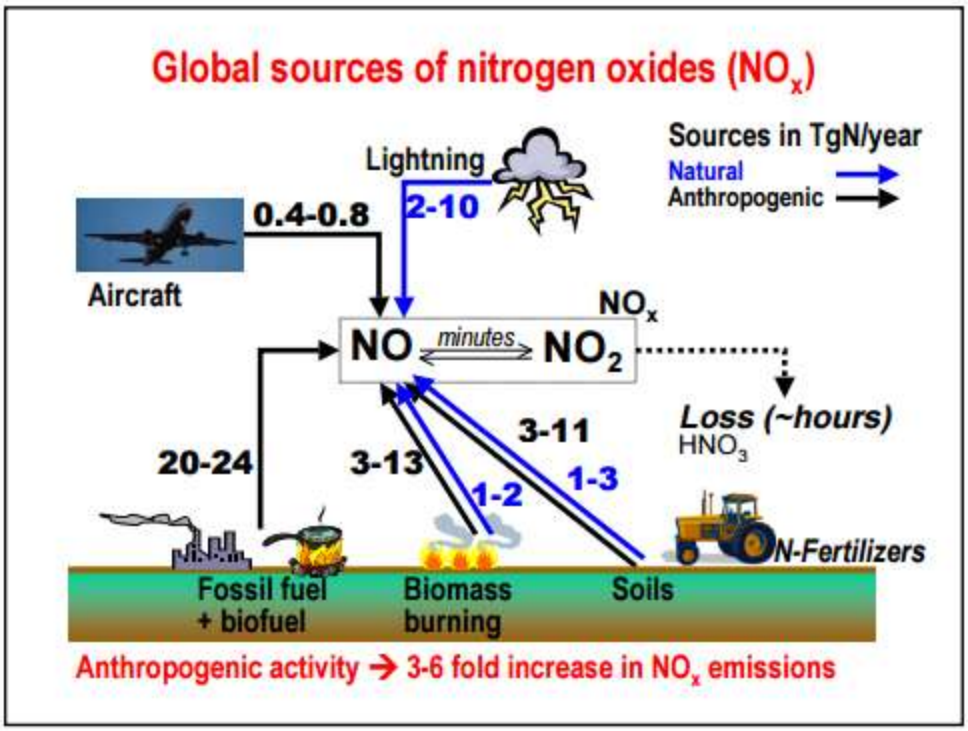

FIGURE 2: PERCENT DISTRIBUTION OF NO_x EMISSION SOURCE (GLOBAL NITROGEN OXIDES INVENTORY)[23]

These trace gases are further categorized into two pollutants, namely: Primary Pollutants and Secondary Pollutants.

Primary Pollutants. These are trace gases which are released directly into the atmosphere from their sources. Examples are SO_2, NO and CO.

Secondary Pollutants. These trace gases are born into the atmosphere as a product of chemical and/or physical transformation of primary pollutants. Examples are ozone, NO_2, CO_2 etc.

2.3 Basic Photochemical Cycle of NO_2, NO, and O_3

When NO_2 is present in the atmosphere with the solar radiation of appropriate wavelength (< 424 nm), ozone formation occurs due to the photolysis of NO_2 catalyzed by the solar radiation,

$$NO_2 + h\upsilon \rightarrow NO + O \tag{2.3}$$

$$O + O_2 + M(N_2, O_2, etc) \rightarrow O_3 + M(N_2, O_2, etc) \tag{2.4}$$

where h and υ are plank's constant and photon frequency respectively. The product these two quantities gives the solar radiation energy needed to photolysize NO_2. M represents N_2 or O_2 or another third molecule that absorbs the excess vibrational energy, and as a result stabilizes the O_3 formed. The only significant source of ozone in the ground surface is through the equation (2.6) [21].

Once O_3 is formed, it reacts directly with NO in the atmosphere to regenerate NO_2,

$$O_3 + NO \rightarrow NO_2 + O_2 \tag{2.5}$$

During daylight hours, the interconversion between NO, NO_2 and O_3 is dominated by reactions (2.3 – 2.5) that equilibrate their concentration in a few minutes (photostationary state) as depicted by equation (2.6)

$$\frac{[NO][O_3]}{[NO_2]} = \frac{J}{K} \tag{2.6}$$

Where J is the rate of NO_2 photolysis which is a function of solar radiation intensity, k is the rate coefficient for NO + O_3 reaction, which is a function of temperature [21].

$$K\ (ppm/\ min) = 3.23 \times 10^3 \exp[-\frac{1430}{T}] \quad (2.7)$$

2.4 Chemiluminescence Technique

Many direct or indirect techniques have been developed for measuring NO_2 in the laboratory and/or in the field. Spectroscopic techniques, for instance, Differential Optical Absorption Spectroscopy (DOAS), Laser Induced Fluorescence (LIF), Cavity Ring Down Spectroscopy (CRDS), Tunable Diode Laser Absorption Spectroscopy (TDLAS) and Resonance Enhanced MultiPhoton Ionisation (REMPI), have been used for selective NO_2 detection [24], [25]. Although some of these methods, such as REMPI and LIF, have very low detection limits, most techniques require considerable operational expertise which are expensive and complex. Thus, the most widely used technique, and at the same time the referenced method recommended by the US EPA [19] and by European legislation [20] for the measurement of NO_2 in monitoring networks is the chemiluminescence technique because of its simplicity.

Chemiluminiscence is the property of some chemicals whereby two chemicals react to for an activated intermediate product, which breaks down to release its energy in the form of photons of light. While the light, in general, can be emitted in ultra violet, infra-red and visible region of electromagnetic spectrum, those emitting visible light are most common [26].

$$A + B \rightarrow AB^* \rightarrow product + h\upsilon \quad (2.8)$$

CHAPTER 3

3.0 EXPERIMENT

3.1 Instrumentation

Two technical instruments were deployed for the purpose of this research work: The EC9841 analyzer from Ecotech was used to perform continuous measurement of concentrations of nitric oxide (NO), total oxides of nitrogen (NO_X), and nitrogen dioxide (NO_2). This device uses gas-phase chemiluminescence property of nitric oxide (NO) to provide accurate measurements of $NO/NO_2/NO_X$ in the range of 0 – 20 ppm with a detection limit of less than 0.5 ppb and resolution of 1ppt, and the Orion weather station from Columbia weather systems which provides ultrasonic wind direction in the range of 0 – 360^o, the accuracy of $\pm 3^o$ and the resolution of 1^o , wind speed in the range of 0 – 60 m/s, the accuracy of ± 3 % for the measurement range 0 – 35 m/s and ± 5% for the measurement range of 35 – 60 m/s and the resolution of 1 m/s, temperature range of – 52 ^{o}C to 60 ^{o}C, with accuracy of ± 0.3 ^{o}C and resolution of 0.1 ^{o}C, relative humidity range of 0 – 100 %, the accuracy of ± 3 % (0 – 90 %), ± 5 (90 – 100 %) and resolution of 1 %, and barometric pressure range of 17.50 InHg - 32.5 InHg, the accuracy of ± 0.015 InHg at 0 – 30 ^{o}C, ± 0.03 at -52 - +60 ^{o}C and 0.01 InHg resolution.

3.1.1 Principle of Operation-NOx Analyzer

The EC9841 analyzer uses gas-phase chemiluminescence detection to perform continuous analysis of nitric oxide (NO), total oxides of nitrogen (NO_X), and nitrogen dioxide (NO_2). The EC9841 design represents an advance in nitrogen oxides analysis technology achieved primarily by using adaptive microprocessor control of a single

measurement channel. The instrument consists of a pneumatic system, NO_2-to-NO converter (molycon), a reaction cell, detector (photomultiplier), and processing electronics.

The analysis of nitrogen oxides by chemiluminescence is generally recommended to be the best direct measurement technique by USEPA. The method is based on the luminescence from an activated molecular NO_2 species produced by the reaction between NO and O_3 in an evacuated chamber. The NO molecules react with ozone to form the activated species NO_2* according to the reaction mechanism:

$$NO + O_3 \rightarrow NO_2^* + O_2 \qquad (3.1)$$

As the activated species NO_2* reverts to a lower energy state, it emits broad-band radiation from 500 to 3000 nm, with a maximum intensity at approximately 1100 nm. Since one NO molecule is required to form one NO_2* molecule, the intensity of the chemiluminescent reaction is directly proportional to the NO concentration in the sample. This radiation is passed through the optic filter to the photomultiplier tube (PMT). The PMT detects the radiation and converts it to a current which is directly proportional to the chemiluminescent intensity.

In order to measure the zero offset of the instrument, a background measurement is performed every 70 seconds by diverting the sample flow from the reaction cell to the cell bypass line. This measurement is electronically subtracted from all subsequent measurements to achieve very stable measurements. The pneumatic system continuously supplies sample air to the reaction cell at a constant rate, allowing the sample to be

measured before exiting the analyzer. The pump pulls a strong vacuum that draws sample air into the inlet and through the particulate filter. The sample flows both directly to the valve manifold (NO port) and through a sample delay coil and molycon to the valve manifold (NO_X port). Within the valve manifold, the critical orifice which maintains constant flow and strong vacuum in the reaction cell. The sample is selected to either come from the NO port or from the NO_X port to the reaction cell via the sample switching valves. Sample then flows to the reaction cell for measurement and out to the external scrubber and pump. Chemiluminescent reaction between NO and O_3 emits broad-band radiation which then converted to electric current by passing it through photomultiplier. The current will then eventually undergo electronic signal processing and be measured as digital values of NO, NO_2 and NOx concentrations. The block diagram for the flow is as shown in the figure 3.

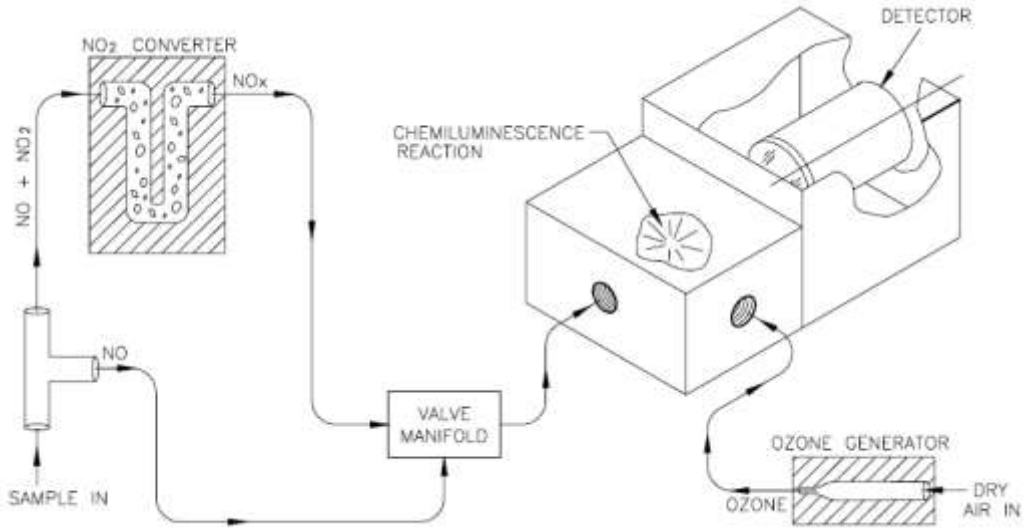

FIGURE 3 : FLOW DIAGRAM OF NO_x ANALYZER [27]

3.1.2 Principle of Measurement- Orion Weather Station

Wind speed and Wind Direction Measurement

Both wind speed and direction are measured by a sensor, using advanced ultrasonic technology. The sensors utilize the ultrasound to determine the horizontal wind reading. The array of three equally spaced ultrasonic transducers on a horizontal plane is an ideal design that ensures accurate wind measurement from all directions without blind angle or corrupted reading. Wind speed and wind directions are determined by measuring the time it takes the ultrasound to travel from each transducer to the other two.

The wind sensor measures the transit time in both directions along the three paths established by the array of transducers. This transit time depends on the wind speed along the ultrasonic path. For zero wind speed, both forward and reverse transit times are the same. With wind along the sound path, the upwind direction transit time increases and the downwind transits time decreases.

The wind speed is calculated from the measured transit time using following formula:

$$V_w = 0.5 \times L \times \left(\frac{1}{t_f} - \frac{1}{t_r}\right) \tag{3.2}$$

V_w = Wind Speed

L = Distance between the two transducers

t_f = Transit time in forward direction

t_r= Transit time in reverse direction

Measuring the six transit times allow V_w to be computed for each of the three ultrasonic paths. The computed winds are independent of altitude, temperature and humidity, which are cancelled out when the transit time is measured in both directions. However, the individual transit time depends on these parameter- temperature, humidity and altitude.

Using V_w values of two array paths is enough to compute wind speed and wind direction. A signal processing technique is used so that wind speed and wind direction are calculated from the two array paths of best quality.

Temperature, Humidity and Pressure Measurement

Barometric pressure, temperature, and humidity measurement are combined in an advanced sensor, tagged PTU module, which is capable of measuring pressure, temperature and humidity as shown in the figure 4. The PTU module contains separate sensors for pressure, temperature and humidity measurement.

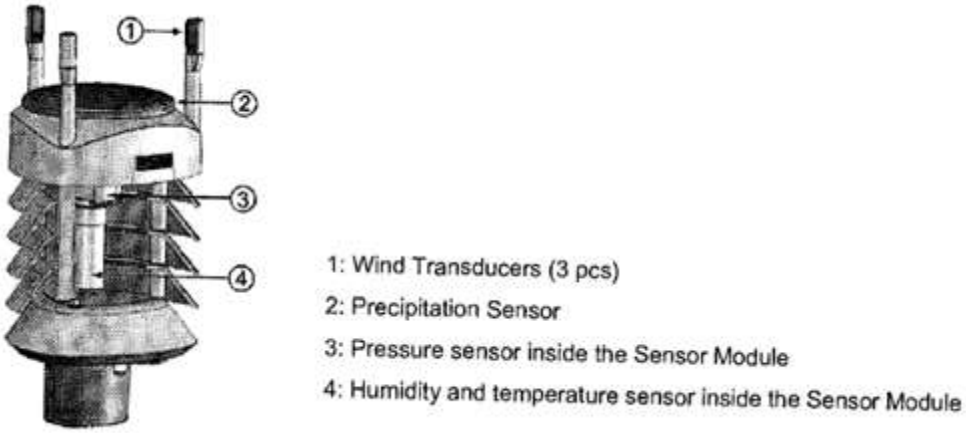

FIGURE 4: CUT VIEW OF WEATHER STATION SENSOR [28]

3.2 Monitoring Location

The location of the monitoring site is situated in KFUPM campus. The choice of this location has a special suitability for this measurement process in that it is within the ring highways which surround the university campus. Figure 5 shows the ring highways in discussion. The monitoring site is bounded in the north by King Abdul Aziz highway, east by King Khalid highway, west and south by gulf cooperative highway which extends from Kuwait city through Saudi Arabia to Bahrain. These highways are always very busy and they carry a large number of motor vehicles at a time. For the highways that form a ring around the monitoring site, regardless of which direction wind blows, traffic emission will definitely be measured in it (monitoring site). In addition to this ring highway, there are quite a number of local roads within the university campus and Dhahran environment which could also be monitored by this monitoring site.

Furthermore, as much as the monitoring site location is central around the highways in Dhahran, so is it to its neighboring cities. Dammam is around 25 km, Khobar is around 5 km and Jubail; which hosts many petrochemical industries, is about 100 km away from Dhahran. With the dispersion and transport by wind, the measurement of NO_x in KFUPM monitoring site can represent the NO_x trend in all those neighboring cities as well. Based on these reasons, the choice of this monitoring site location is at advantage to getting scientifically reliable data for NO_x analysis which truly would reflect the correct level of these gas pollutants in the ambient air of these aforementioned cities.

FIGURE 5: MAP OF THE RING HIGHWAY AROUND THE MONITORING SITE [29]

3.3 Methodology

The set-up for air sample extraction for the experiment was carried out in Building 28, (Energy research center), on top of the building precisely, about 10 m from the ground. This monitoring site was chosen because of its close proximity to the traffic route since traffic emission has been suspected majorly for high NO_x episode in most urban areas [13], which Dhahran is never an exception. Furthermore, setting up the experiment at a certain height clears off the possibility of air mass flow being obstructed either by another tall building or trees, because the monitoring site is the tallest building in the vicinity. As such, there was no doubt as to the air sample getting into the instruments for the measurement.

Both weather station and air sample collector, linked through pipe into the NOx analyzer, kept in the laboratory, for continuous supply of air sample, were mounted at the monitoring site for the period of 3 months both night and day. The weather station was placed facing north for measurement of meteorological data (Temperature, Pressure, Humidity, Wind Speed and Wind Direction). The air sample collector oriented with its surface perpendicular to the air flow direction to ensure proper intersection and enough air sample getting into our system. To prevent tiny air particle from getting into the analyzer, 5 microns filter, in addition to the internal filter in the NO_x analyzer, is applied at the surface of the collector whose pore size can only permeate air not tiny sand particle that was prevalent due to sand storm in the month of May when the measurement started.

Through wireless system, weather station established a connection with PC, in the laboratory, for its data logging from the top of the building into the monitoring PC.

To ensure integrity of data, calibration of NO_x analyzer and daily maintenance for both devices were carefully carried out in line with the USEPA recommendation on quality assurance and quality control.

3.3.1 Data Acquisition and Analysis

The process of data acquisition took place for the period of four months (07^{th} of May, 2015 to 30^{th} of July, and it started with the calibration process for NO_X analyzer with NO_2 standard source (2.6 ppm) of known concentration and the device was found to give accurate measurement with acceptable error limit. The reason for this calibration is to ascertain that the analyzer readings are correct, reliable and free of error due to the recalibration process as the device is prone to calibration error whenever it is moved from one location to another.

To condition weather station and NO_X analyzer to log in data simultaneously with the same time stamp for NO, NO_2, NO_X, temperature, pressure, humidity, wind speed and wind direction after every second in the same data file, "LabView Program" was written and employed to synchronize these two devices for the same acquisition time and automate the whole process of the data acquisition.

From this data, which was indeed a large volume of data, average hourly, average daily and average weekly concentrations were computed through the aid of Mathematica program. These computed averages were used for the purpose of the analysis. The flow chart of the acquisition process is as shown in figure 6 below.

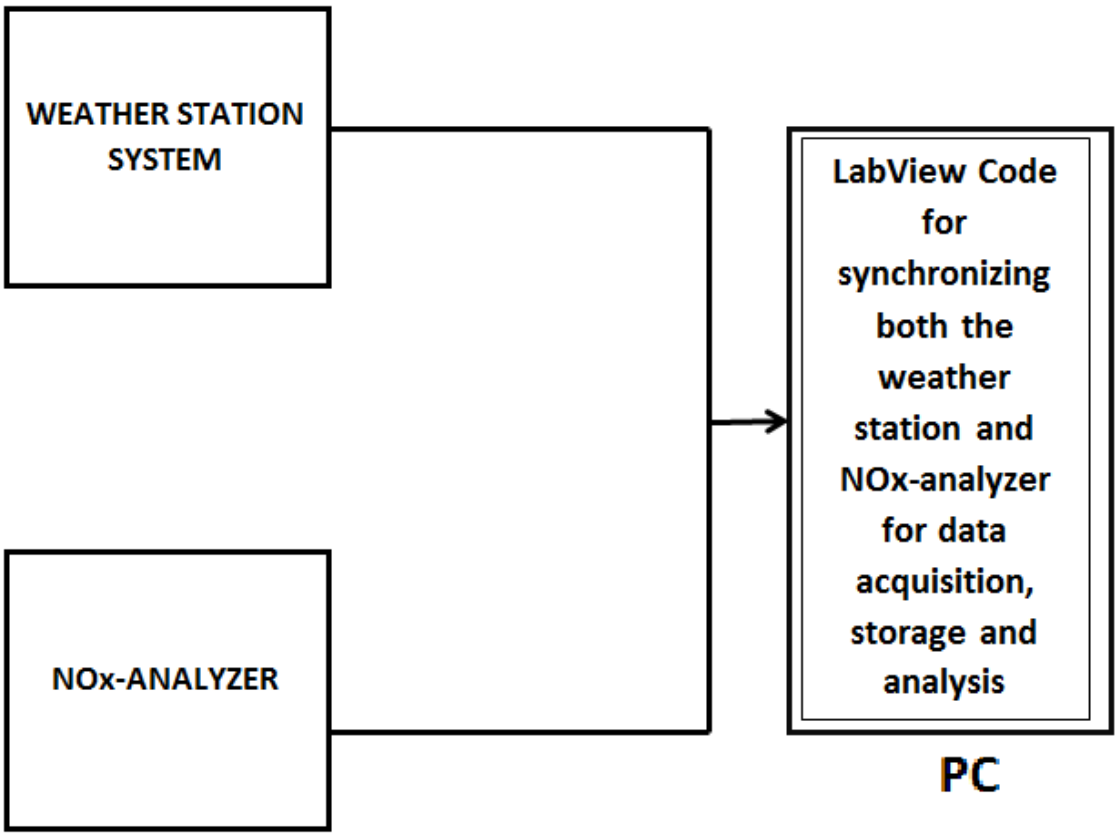

FIGURE 6: FLOW CHART FOR DATA ACQUISITION PROCESS

3.4 Mathematical Modeling

Application of Mathematical models to the analysis of urban pollution episodes has been instrumental in establishing the relationship between pollutant source–receptor. Establishing this relation, will aid in developing optimum emission control strategies for gas pollutants. A multitude of numerical advection schemes have been tested and compared, which proves the suitability of mathematical models for use within air quality models [18], [30], [31].

Mathematical models employed in air pollution are classified, in general, into two groups: models which depend on the statistical analysis of previously acquired data, and models which rely on theories related to chemical processes and atmospheric movements. Long-term data are used in statistical empirical model to evaluate the possibility of pollution formation. Meteorological and chemical processing data are not used directly in these models to calculate the possibility of pollution formation.

The second type of model makes use of continuity equations written for each type of air pollutant. These models assemble the effects of all dynamic processes in one equation, such as chemical reactions and turbulent diffusions, which influence the mass balance in the control volume of air. The data on emission, meteorology and atmospheric chemistry are used as input data in these models. This model can be written for either dynamic or steady states. The wind speed, wind direction, temperature, humidity and solar radiation, depending on height, are acquired as the meteorological information. Pollutant concentration can be predicted according to the time and coordinates by means of these models. The validity of the model is tested by comparing the observed and predicted data [21]. Other studies involved dispersion models of pollutants from fixed sources [32]. These models are usually very complicated to be applied, especially in an area of

complex topography. Therefore, simple air quality models based on emission and meteorological data have been proposed [30].

In this research, the semi-empirical model which was formulated by previous studies [30] has been applied to the NOx pollutants as against SO_2 for which it was initially devised. The air volume over the city of Dhahran has been used as a control volume and a mass balance in this control volume has been put under consideration.

This model assumes a simple box for the city as shown in figure 7, within it, the pollutants emanated which then get dispersed and transported by meteorological data.

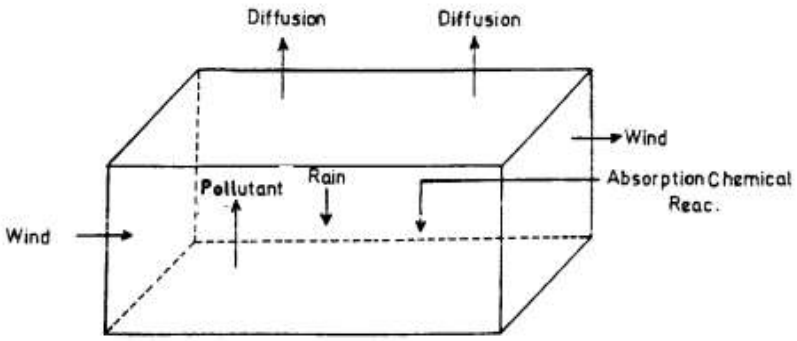

FIGURE 7: CONTROL VOLUME OVER THE CITY OF DHAHRAN AND INPUT-OUTPUT PARAMETERS [30]

Model Assumptions

To further simplify the model, the following assumptions were made as regard the validity of the model:

(1) It is presumed that the mountains or tall buildings or trees around the city did not pose topographic barriers for the wind entering and leaving the control volume in all directions.

(2) Diffusion caused by temperature differences between the control air volume and upper layers of the atmosphere is assumed to be negligible.

(3) Since the reaction mechanisms of the pollutants in the atmosphere are complex, these effects were not considered in detail. Instead, it was supposed that the exit rate of pollutants from the control volume by absorption and chemical reaction was proportional to the concentration

(4) The monitoring site is surrounded by ring highway, so there is no preferred direction for wind to blow; all directions are equally probable.

With regards to these assumptions made above, the mass balance of control air volume may be written as follows:

Accumulation rate in control volume is given by equation (3.3)

$$V.\frac{dC}{dt} = \sum entry\ rate - \sum exit\ rate \tag{3.3}$$

Where V is the controlled air volume, C is the pollutant concentration

Each of these terms can be separately evaluated as follows:

** Entry Rate Term:

Since in this region it has been established that the major source of NOx emission is basically traffic emission. Hence the emission source which will be catered for in this model is traffic emission source. This emission source (traffic) is due to the burning of fuel within automobile engines and through release of combustion waste, many gas pollutants get into the atmosphere. Based on this, pollutant entry rate is proportional to the daily used fuel, Q,

Q supplies steady heat loss and is given by popular well-known heat transfer equation:

$$H_o = UA\Delta T \tag{3.4}$$

where H_o is the total calories needed for heating the city; U is the average total heat transfer coefficient; A is the total heat transfer area of the city; and ΔT is the difference between outside city temperature and inside city temperature, $\Delta T = T_r - T$

$$\text{NOx emission rate} = H_oK \tag{3.5}$$

where K is the NOx emission factor which has been defined for different gas pollutants by US EPA. Therefore pollutant entry rate:

$$\text{NOx emission rate} \propto KUA(T_r - T) \tag{3.6}$$

This can be rewritten as:

$$\text{Pollutant entry rate} = a - bT \tag{3.7}$$

where $a = KUAT_r$, $b = KUA$

Also relative humidity which is the measure of water vapor in the atmosphere contributes in its own quotas to the NOx pollutant in the atmosphere. Relative humidity is usually high in the night when the atmosphere is stable and vertical mixing is not strong. All these aid the retention of pollutant in the atmosphere. Thus, the entry rate of the pollutant due to relative humidity is proportional to the relative humidity of the air in the atmosphere, i.e $\propto \quad H$.

** Exit Rate Terms:

Exit rate with the wind is proportional to average wind speed (S (kph)).

Also exit rate with absorption, chemical reactions and eddies (diffusion) which are capable of undermining the NOx concentration by either absorbing the pollutant or transforming it through chemical reaction, though the process is very complex, its effect on NOx can be summed up as being proportional to the concentration of the pollutant in the atmosphere, i.e diffusion $\propto$ pollutant concentration (Cj) in the atmosphere.

When the above terms are introduced in equation (3.3) we obtain:

$$V.\frac{dC}{dt} \sim V.\frac{\Delta C}{\Delta t} = a_o - a_1 T + a_3 H - \left(a_2 S + a_4 C_j\right) \quad (3.8)$$

As ΔC= $C_j - C_{j-1}$ and Δt = 1 day, when equation (3.8) is rearranged, equation (3.9) below is arrived at:

$$C_j = A_o - A_1 T - A_2 S + A_3 H + A_4 C_{j-1} \quad (3.9)$$

where $A_i = \frac{a_i}{V}$, $i = 0 - 4$ and $A_i s$ are model parameters.

In equation (3.9), j denotes the actual day and j-1, the previous day. Hence, this model establishes the relation between actual NOx concentration C_j with the actual meteorological parameters, T, H, S and previous day concentration.

To evaluate the model parameters, meteorological data and NOx concentrations measured in the monitoring site are fit to this equation using linear regression model.

CHAPTER 4

4.0 RESULTS AND DISCUSSION

4.1 Meteorological Condition

The basic meteorological conditions registered in the current study are wind speed, wind direction, ambient air temperature, relative humidity and atmospheric pressure. These paremeters were measured so as to evaluate the effect they might have on NOx concentrations.

Hourly mean value of every data acquired within each hour of the day for temperature (^{o}C), relative humidity (%), pressure (InHg) and wind speed (mph) at the monitoring station from May to July 2015 are computed and shown in figures (8a) – (11a). Figures (8b)-(11b) depict the hourly variations of these meteorological parameters for every day of data acquisition.

The maximum temperature of approximately 39 ^{o}C was recorded between 12 PM and 2 PM , while the minimum temperature (31 ^{o}C) occurs at around 6 AM in the morning. A rapid increase is observed between 6 AM and 12 PM and this is maintained for almost 2 hours after which it starts to decrease again to approximately 33 ^{o}C at around 12 PM. This same level of decrease continues till 6 AM the following day just as shown in figure 8(a). This temperature curve is typical of summer temperature distribution characterised with intense midday temperature.

Figure 9(a) shows hourly variation of relative humidity, whose data was acquired during summer (May – July 2015). The highest relative humidity was registered between 12 AM and 1 AM , wheareas the minimum was observed around 12 PM. This seems

behaving conversely to what is observed with temperature curve. This temperature-humidity relation is a common knowledge, though the reverse is possible, when the high humidity may imply higher temperature, depending on the season of the year in discussion.

Furthermore, hourly average of wind speed is also plotted in figure 10(a) where the steady rise in the wind speed is observed from 1 AM and reaches maximum speed at around 3 PM. Shortly after, it starts to drop until it reaches lowest ebb at 11 PM. This rise and fall of the wind speed is evidently in connection with the values of other meterological parameters such as temperature, relative humidity etc… as they have influence on it.

A little fluctuation is observed with air pressure measured within May and July 2015. After computing the hourly average, the plot is presented in figure 11(a). It is virtually constant through out the measurement period as the maximum pressure measured is 29.4 InHg while the minimum is 29.35 InHg- just differrence of around 0.05 InHg. Therefore, the effect of pressure can be declared inactive for this period.

Figure 12 is a single plot illustrating how the four variables (temperature, humidity, wind speed and pressure) correlate with one and another. It is obvious, from the figure that pressure is almost constant throughout the day and no noticeable effect does it possess over the other parameters. Temperature and wind speed on the other hand, are quite interconnected as their both curves show a similar shape and both reach the maximum around same period (1 – 3 PM). This behavior is very much expected as the air temperature, due to the heating of air close to earth surface, is a deterministic factor that determines how strong and to which direction wind blows. Hence, wind which is due to

the variation of pressure (stress) created by non-uniform absorption of solar energy radiation across the earth surface, gives swift response to temperature changes as the case observed in figure 12. However, relative humidity as seen from this figure has never deviated from what is expected – counter- behavior to the temperature change. The increase in temperature is accompanied with the decrease in relative humidity and vice versa. In fact, temperature, which reaches its maximum value around 12 AM, also the same time the relative humidity, reaches its lowest ebb and the trend continues as shown in the figure.

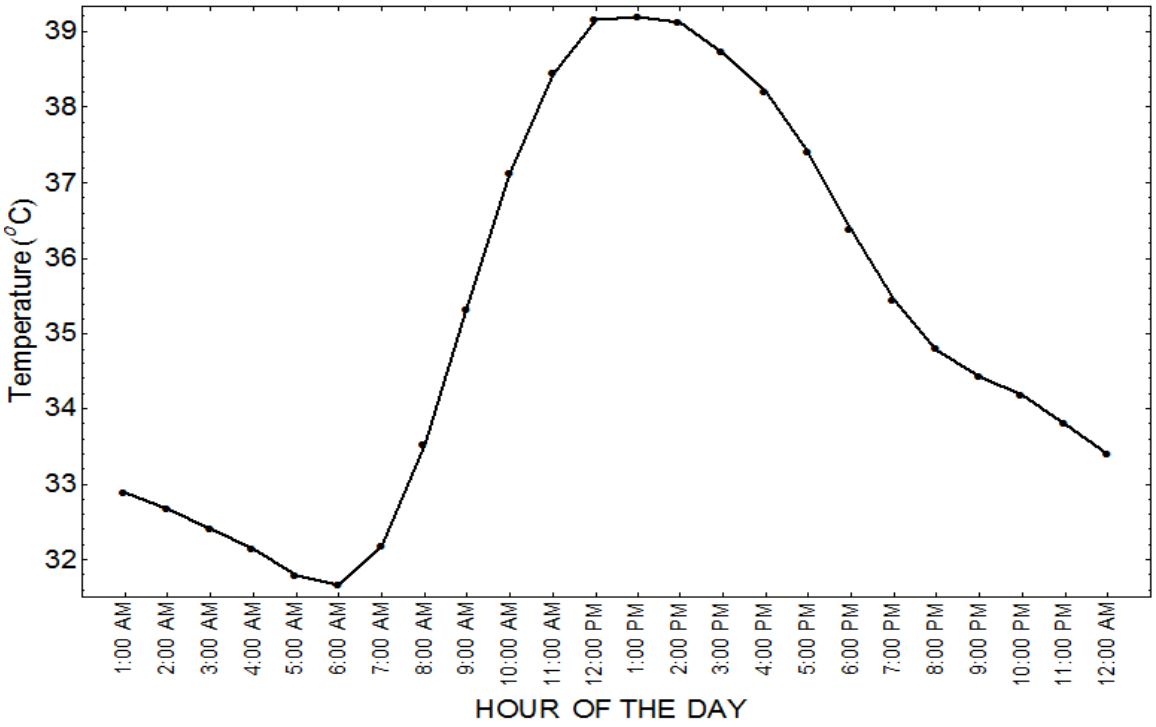

FIGURE 8 (A): DAILY HOURLY AVERAGE VARIATION OF TEMPERATURE FOR DATA FROM MAY TO JULY

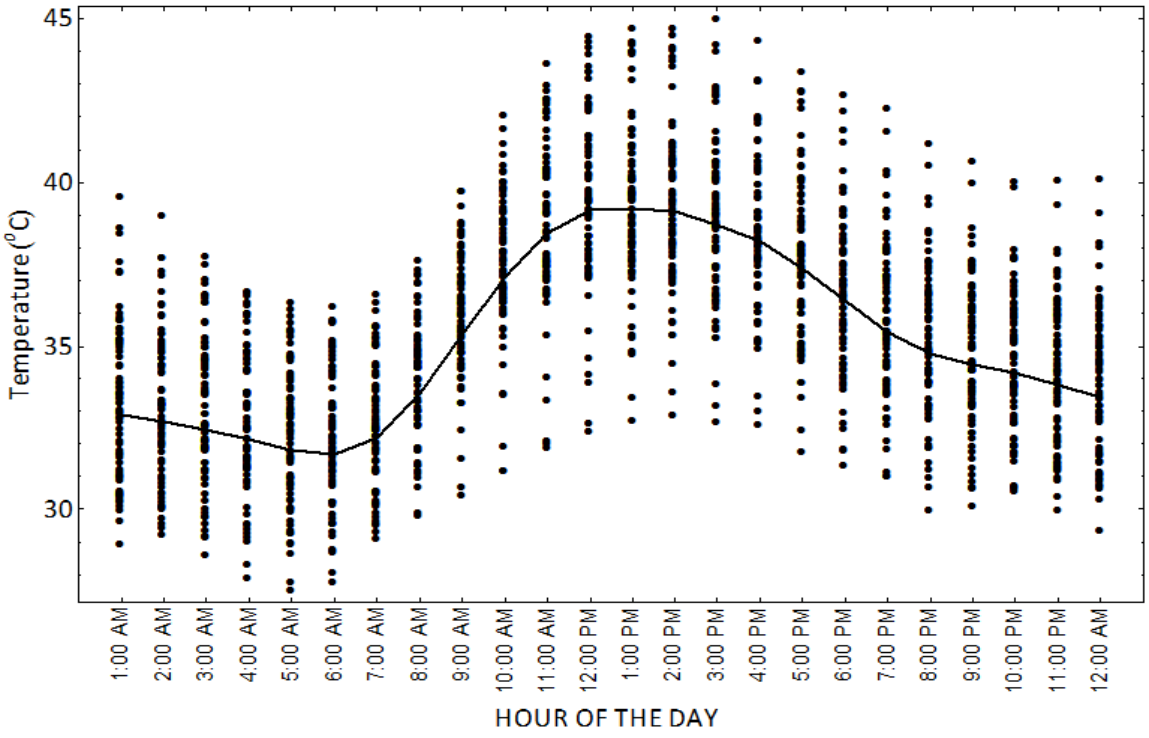

FIGURE 8 (B): HOURLY AVERAGE TEMPERATURE FOR EACH DAY OF DATA ACQUISITION FROM MAY TO JULY

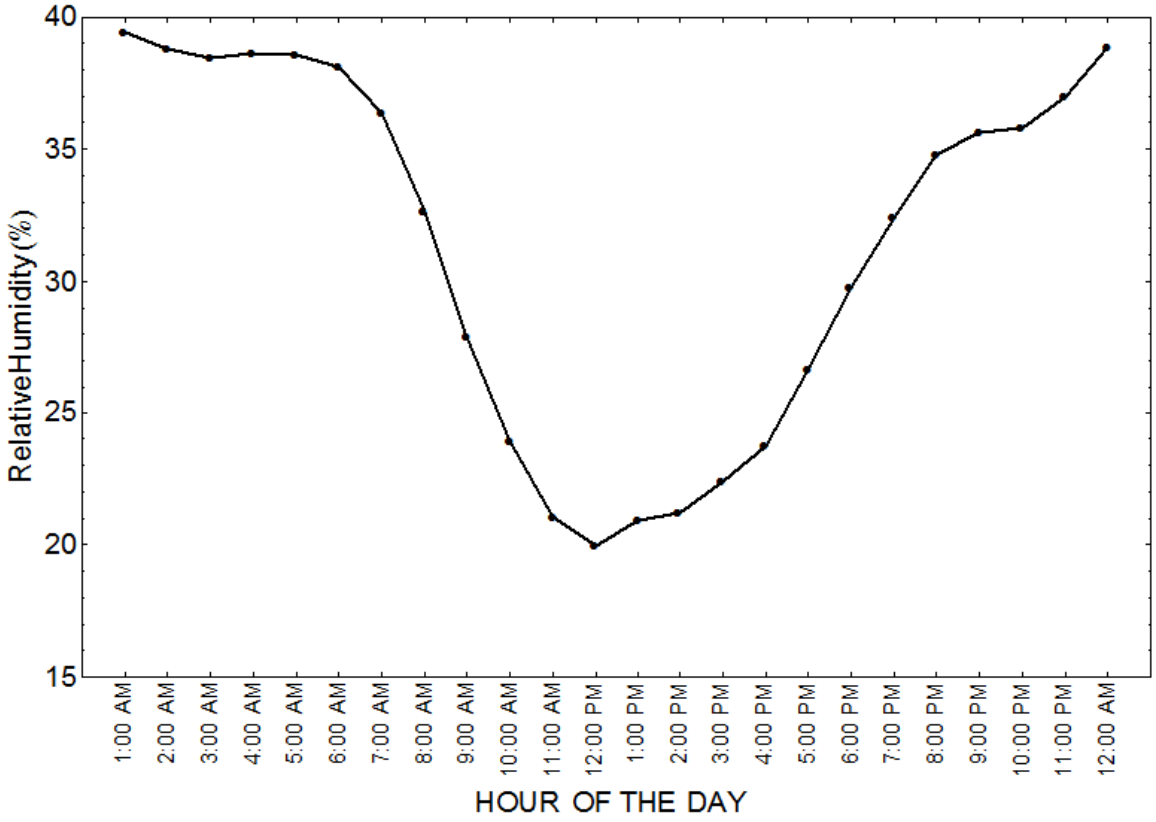

FIGURE 9 (A): DAILY HOURLY AVERAGE VARIATION OF RELATIVE HUMIDITY FROM MAY TO JULY

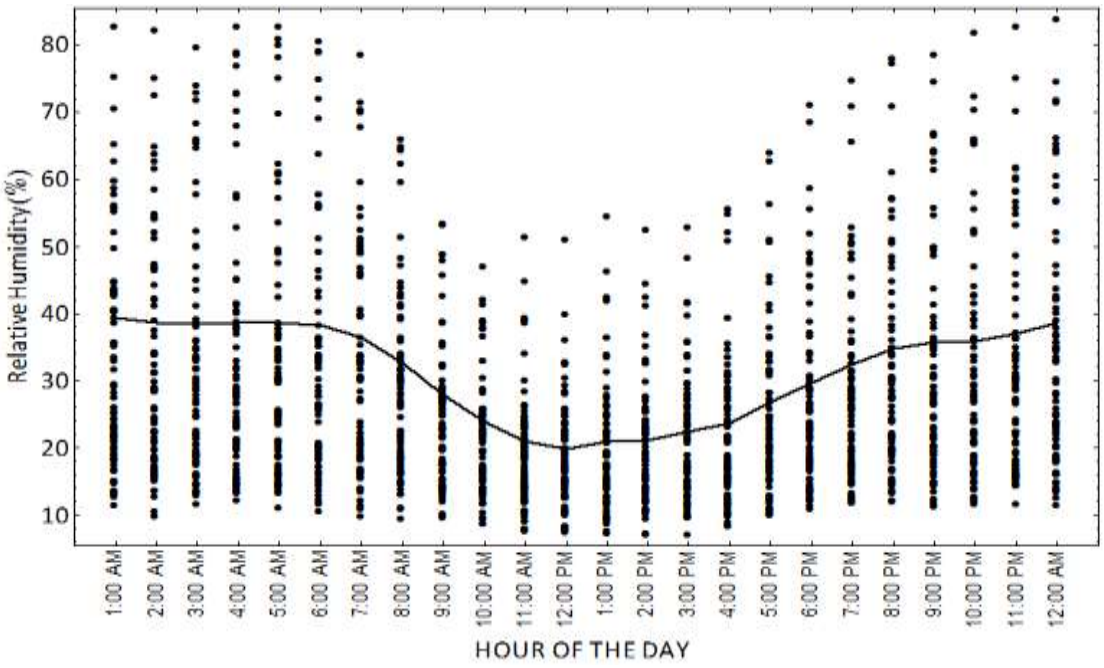

FIGURE 9 (B): HOURLY AVERAGE RELATIVE HUMIDITY FOR EACH DAY OF DATA ACQUISITION FROM MAY TO JULY

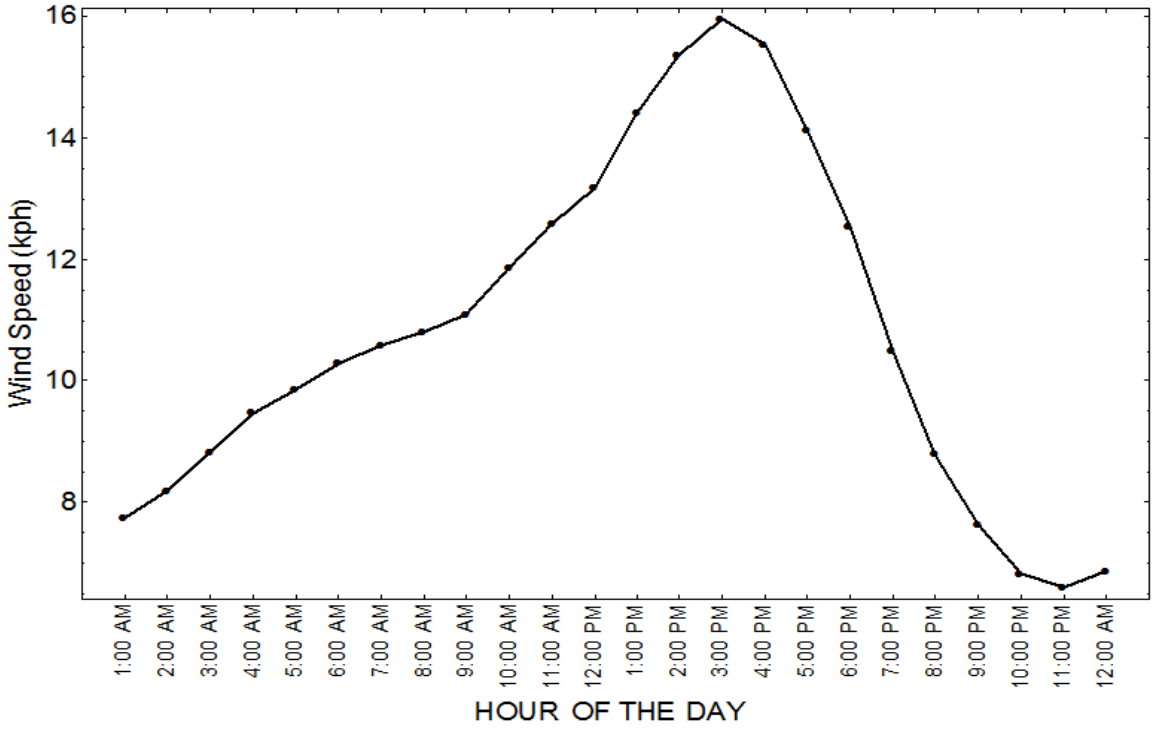

FIGURE 10 (A): DAILY HOURLY AVERAGE VARIATION OF WIND SPEED FROM MAY TO JULY

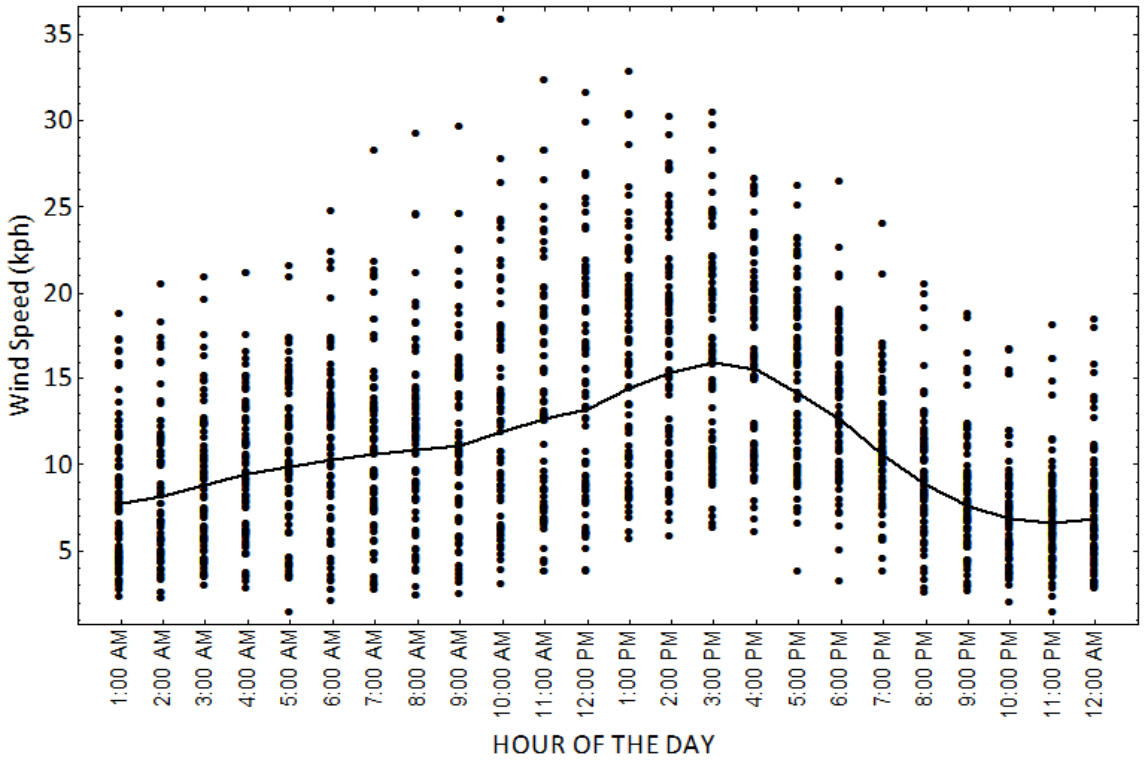

FIGURE 10 (B): HOURLY AVERAGE WIND SPEED FOR EACH DAY OF DATA ACQUISITION FROM MAY TO JULY

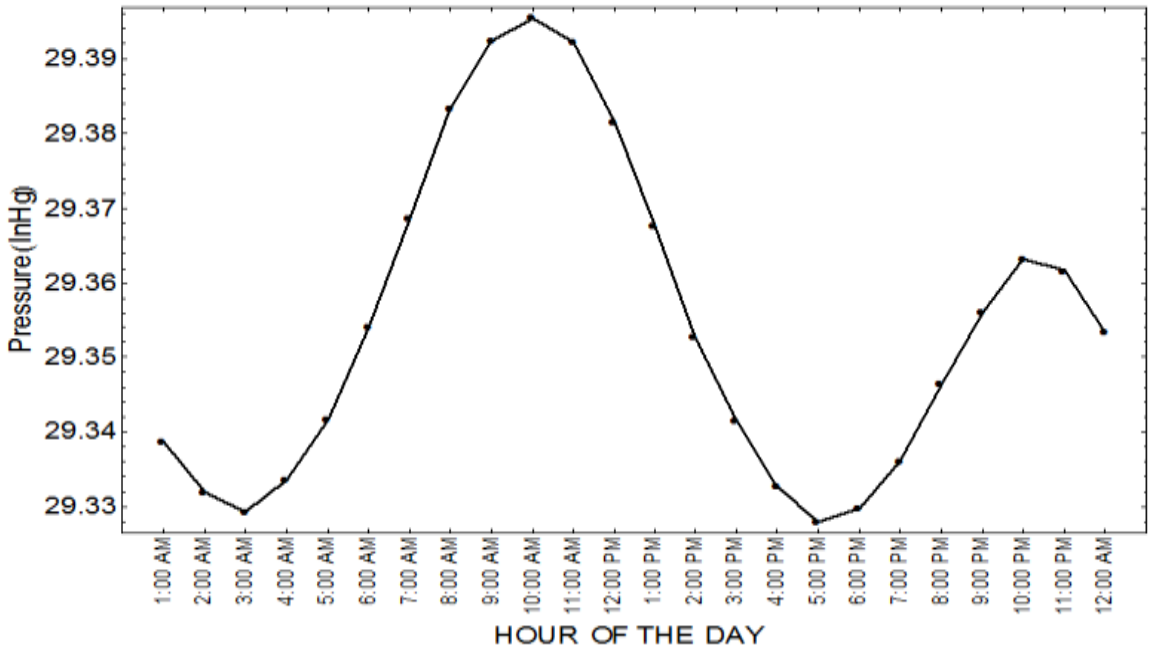

FIGURE 11 (A): DAILY HOURLY AVERAGE VARIATION OF PRESSURE FROM MAY TO JULY

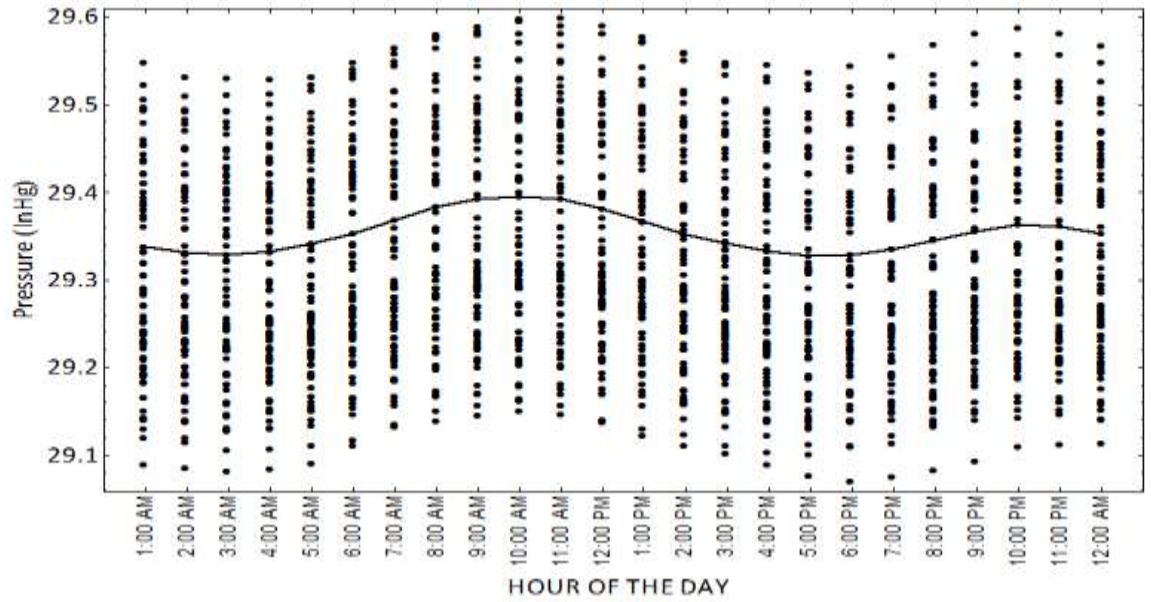

FIGURE 11 (B): HOURLY AVERAGE TEMPERATURE FOR EACH DAY OF DATA ACQUISITION FROM MAY TO JULY

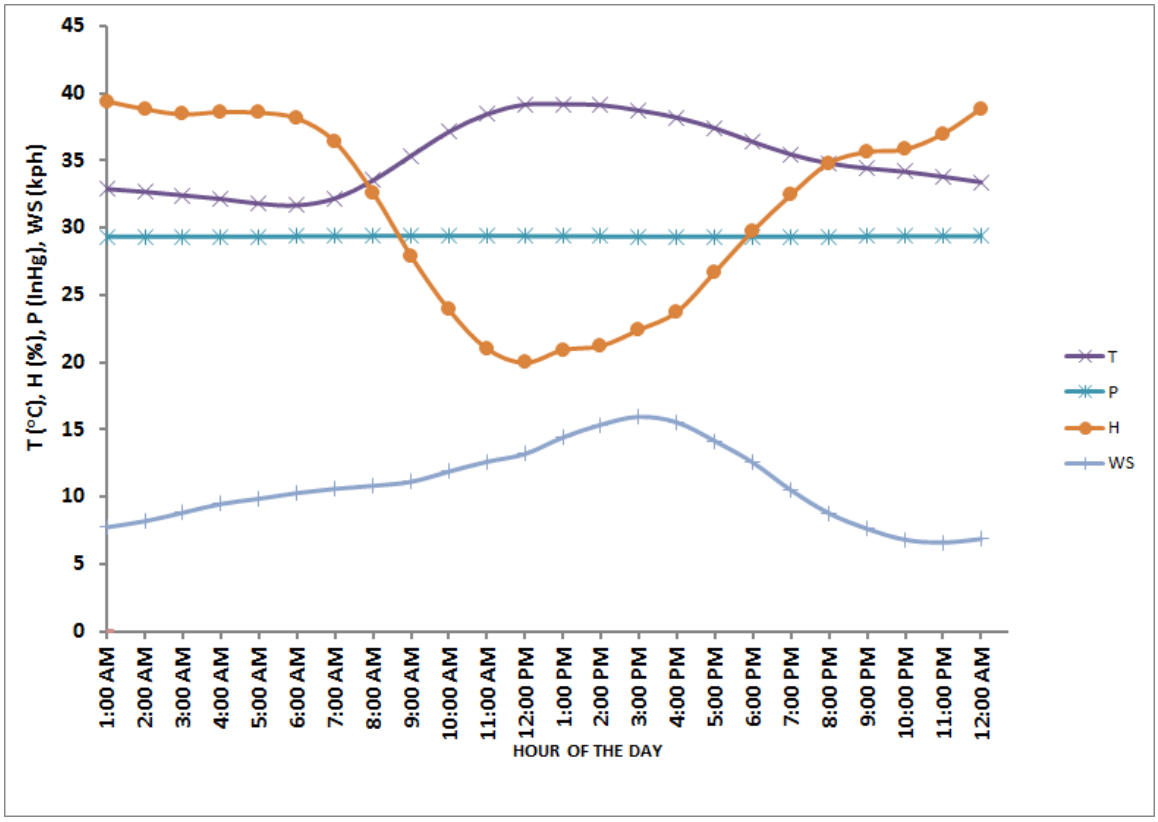

FIGURE 12: COMPARISON OF HOURLY AVERAGE VARIATION OF TEMPERATURE, HUMIDITY, WIND SPEED AND PRESSURE

4.2 Daily Hourly Average Concentrations of NO, NO_2 and NO_X

Figures (13a)-(15a) show the daily hourly variation of NO, NO_2 and NO_X concentrations, figures (13b)-(15b) is the plot of hourly average concentrations of NO, NO_2 and NOx for each day of data acquisition while figure 16 is the comparison plot of these pollutants, in the ambient air for the data acquired from month of May till July. The hourly average concentration is computed by averaging the data, which was hitherto acquired every second during the acquisition process, for every hour, reducing the whole huge data to 24 data points plotted against their corresponding hour of acquisition as in the figures (13a)-(15a) and figure 16 below. In other words, the plots depict the concentrations (ppb) on vertical axis plotted against hours of the day (1 AM – 12 AM) on the horizontal axis. The daily cycle of these concentrations in urban atmosphere of this area is observed to be strongly influenced by traffic emission, photochemistry activities and planetary boundary layer height.

From figure 13(a), the highest hourly average concentration of the primary pollutant, NO, was observed at 8:00 AM at the monitoring site in Dhahran. In the early morning, around 5:00 AM, the NO concentration rises and reaches a maximum point during rush hours, when the human activities-hustling and bustling and traffic emissions- are at the high ebb. So soon around after 8 AM, the concentration begins to descend, marking a reduction in traffic emission as people have already settled down in their various offices for normal routine assignments. This is an evidence that majority of people plying these highways are mostly workers who try to keep up with statutory 8 o'clock resumption at their places of work.

This reduction in NO concentration continues until 9 PM in the night, though some period within this time range coincides with the closing hour of workers, which is initially expected that the NO concentration should distinctively rise again, this is however not the case, a very diminutive bump was observed (quite smaller than expected) around 5 PM coinciding with the period of exodus of workers, after closing from their places of work. The reason for this deviation is probably due to the continuous formation of ozone by NO_2 photolysis (photochemical reaction) since temperature (which is an important parameter in NO_2 photochemical reaction) is expected to be intense during this period. And this ozone, at the ground surface level is very efficient in transforming NO to NO_2 via equation (2.5). Consequently, as soon as NO from the traffic emission gets into the ambient air, they are quickly converted, by ozone formed through equation (2.4), before reaching the monitoring site, to NO_2 as illustrated in equation (2.5), which then get registered by monitoring device. Once again, around 9 PM, NO concentration begins to rise, coinciding with the evening traffic flow (lower concentration than the morning concentration) as it is common practice in Dhahran that human activities extend to this period in the nighttime.

Conclusively, it can be inferred from figure 13 that NO concentration, while other sources are not impossible, depends mostly on traffic emission, though it may be seriously affected by other natural atmospheric processes which may possibly influence in a very complex and complicated manner.

As regards NO_2 concentrations, the data acquired in the region of interest is analyzed and depicted in figure 14(a) and also figure 16 for comparison purpose with NO and NO_X. NO_2 level rises and attains peak around 9 AM in the morning (1 hour after NO reaches its

morning peak, approximately around 8 AM). The retarding moment between the formation of peak concentrations of NO and NO_2 is lending credence to the fact that NO_2 is partially formed from NO. Moreover, NO_2 second peak also appeared at 11 PM in the night. The second peak in the night is observed, as reverse to observation with NO peaks, to be higher than the early morning peaks. This discrepancy may be owing to the large presence of ozone, formed during afternoon, in the night which reacts with NO from traffic emission to produce more NO_2 than in the early morning time when the ozone level is minimal. In addition, NO_2 is more stable in the night as there is no solar radiation to photolyze it to produce ozone. Moreover, the planetary boundary layer height is expected to have fallen during this time because of the stability of the atmosphere due to the fall in the temperature which then seals the pollutants to the Earth's surface. Hence higher concentration of NO_2 registered in the nighttime is as expected and justified.

NO_X is the total sum of NO_2 and NO concentration in the atmosphere, which is emitted by various sources (biogenic, vehicles, industries, etc …..). The emission of this pollutant into the ambient air takes majorly the form of NO which is later oxidized by different photochemical paths, in fact more than 95 % of the NO_X originated from NO. NO_X reacts in the presence of volatile organic compounds (VOCs), chemical products formed due to the incomplete combustion of fuel in automobile engines, and sunlight to yield ozone and other secondary pollutants through the equation (4.1):

$$\text{VOCs} + NO_X + h\nu \rightarrow O_3 + \text{PAN} + \ldots\ldots\ldots \quad (4.1)$$

Concurrently with the VOCs oxidation in the lower atmosphere, NO is oxidized to NO_2 by the peroxy radicals formed, and O_3 is generated through equation (2.5) and (2.6).

As depicted in figure 15 (a), NO_X is not behaving more differently than NO_2; it reaches its minima and maxima same period of time as NO_2. This is not unconnected with the fact that in this region- Dhahran- NO and NO_2 are the prominent nitrogen oxides present in the atmosphere, though the presence of some other nitrogen oxides is not ruled out, their quantity is too minute for our detector to measure. As a result, NO_X only comprises the sum of NO and NO_2 concentrations.

As it can be observed in the graphs below, figure (13a)-(15a), NO_2 is more abundant because of its longer resident time than NO in the atmosphere, so higher NO_2 concentrations are measured. This is the reason that NO_2 curve changes with concomitant change in the NO_X concentrations.

Figure 16 compares the behaviors of NO, NO_X and NO_2 measured in the ambient air of Dhahran. From 1 AM both NO and NO_2 are observed behaving approximately similar as both seem to be decreasing to their lowest possible concentrations for the period which occurs at around 5 AM. This reduced concentrations registered during the midnight could be attributed to the dwindling number of automobile on the highway, for almost all human activities have gone to rest for the day, thereby reducing traffic emission which is the major source of NO that translates to NO_2 concentrations. Moreover, the reduction in NO concentrations indirectly leads to the decrease in the concentration of NO_2 measured, since the mostly suspected source of NO_2 during the period is through oxidation of NO by ozone, of which both (NO and ozone) are available at the meager quantities during this time for the reason hitherto stated.

At around 5 AM, NO and NO_2 start rising again until NO reaches the top concentration at 8 AM, the period corresponding to the rush hours of the day. An hour later 9 AM, NO_2

reaches maximum concentration also. NO_2 is lagging behind NO within this period may perhaps be due to the faster rate of NO emission from automobile, while the rate it is being converted to NO_2 is slower because, in the early morning, the ozone concentration required for oxidation of NO to NO_2 is only available in little quantity as the photolysis of NO_2 is not very active during this period [33].

Lastly, while the NO level is found decreasing from 8 AM through to around 9 PM before it once rises again, NO_2 similarly decreases between 9 AM and 11 AM, then rises up again until it reaches the maximum at 11 AM. The contrast in the behavior of NO and NO_2 in this last part of the day (12 AM and 12 PM) is as a result of intense solar energy which catalyzes the production of ozone from VOCs according to equation (4.1) which in turn oxidizes NO from traffic emission promptly into NO_2, thereby reducing NO concentrations measured in the monitoring site and elevates NO_2 concentration until in the night when the level of ozone starts to drop with corresponding decrease in NO_2 also. Consequently, it can be succinctly concluded, through the inference from figure 16, that the level of NO and NO_2 in the ambient air are interwoven.

The reported data and analysis in this research work are consistent with those of numerous studies [12], [13], [34], which report the influence of traffic emissions in the concentration surge of NOx pollutants in the urban cities.

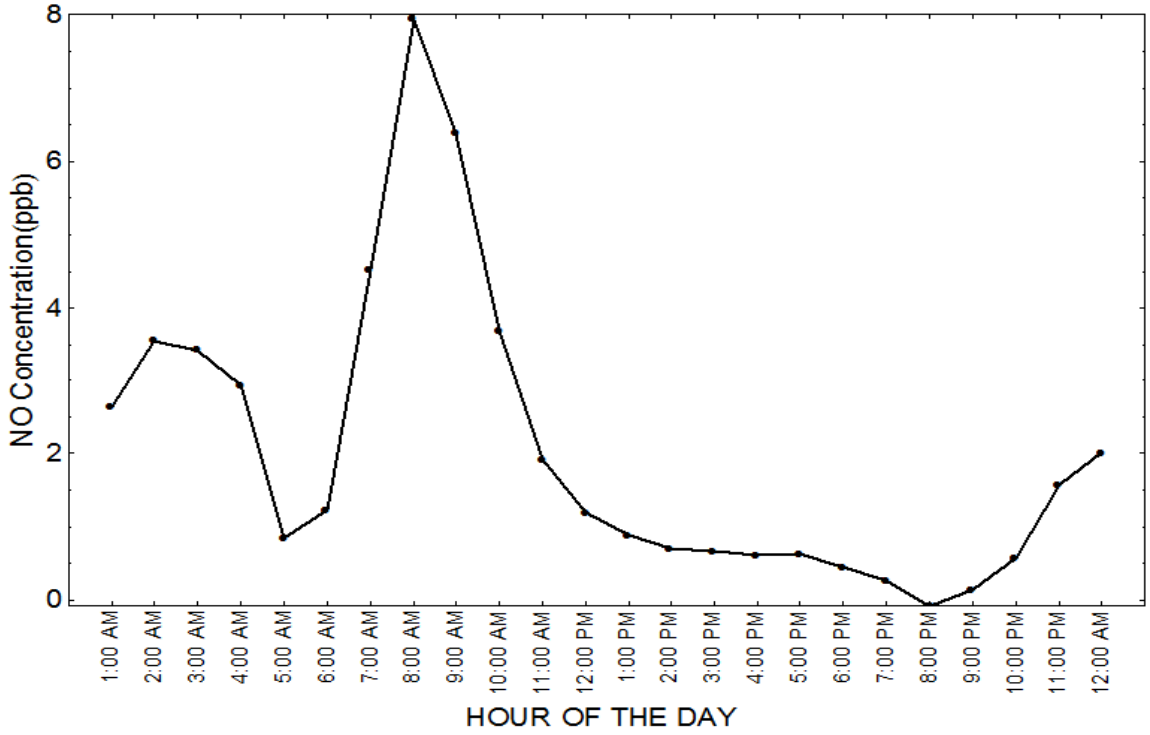

FIGURE 13 (A) : DAILY HOURLY AVERAGE VARIATION OF NO CONCENTRATION IN AMBIENT FROM MAY TO JULY

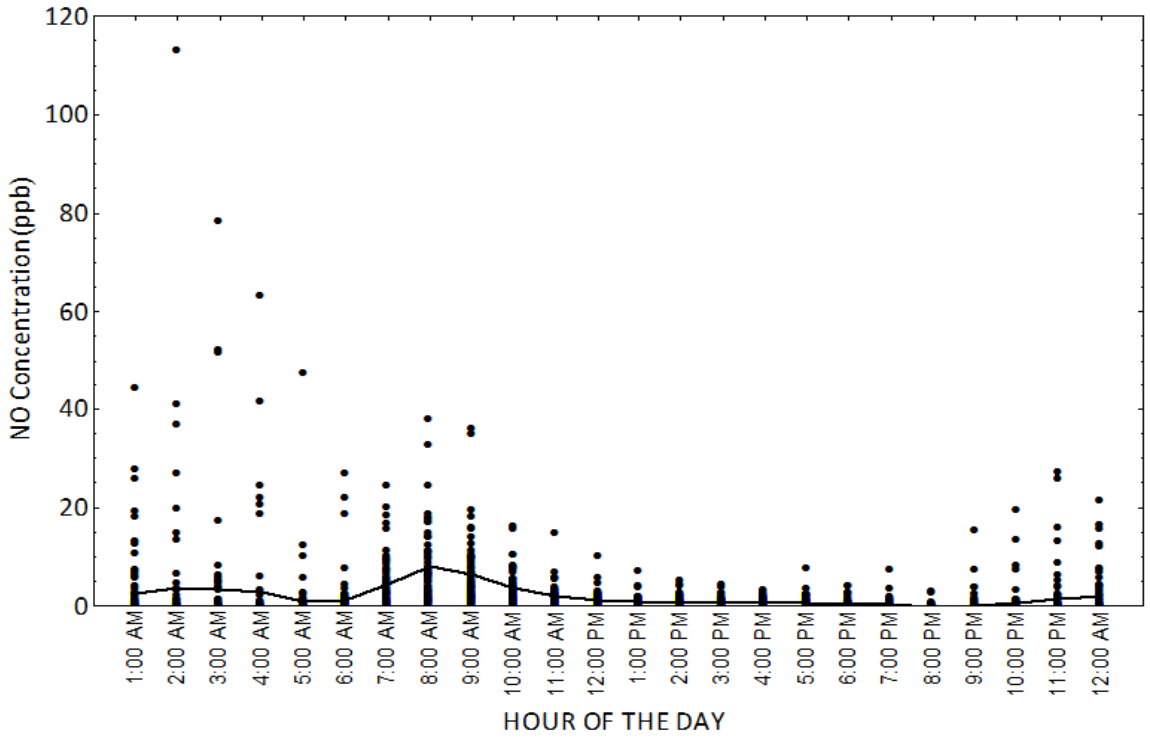

FIGURE 13 (B): HOURLY AVERAGE NO CONCENTRATION FOR EACH DAY OF DATA ACQUISITION FROM MAY TO JULY

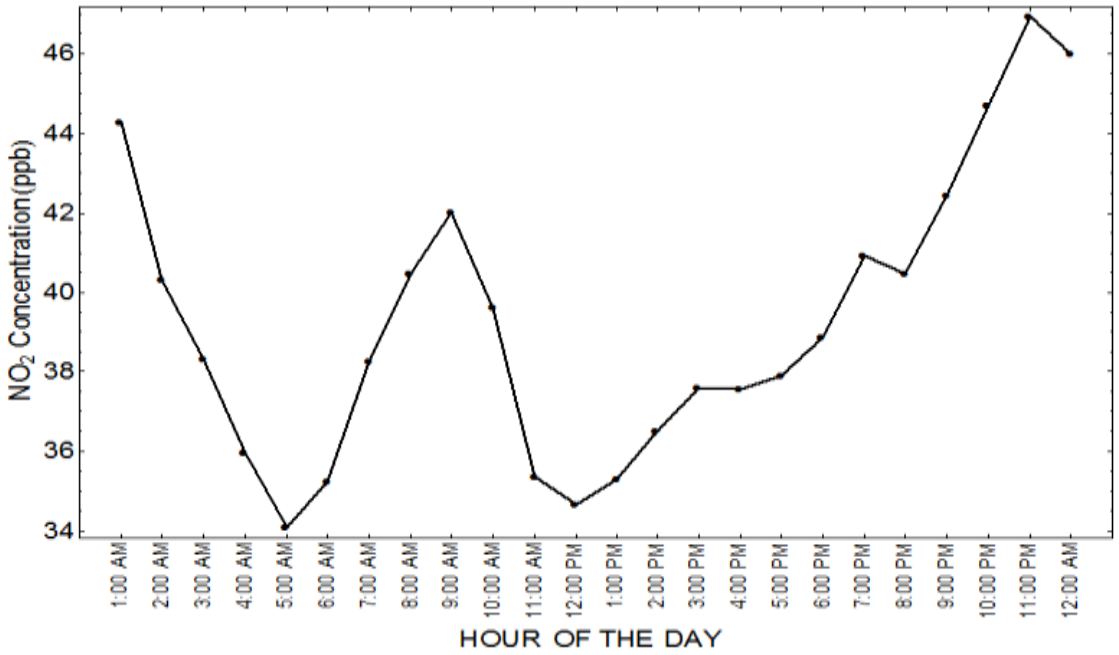

FIGURE 14 (A): DAILY HOURLY AVERAGE VARIATION OF NO_2 IN AMBIENT AIR FROM MAY TO JULY

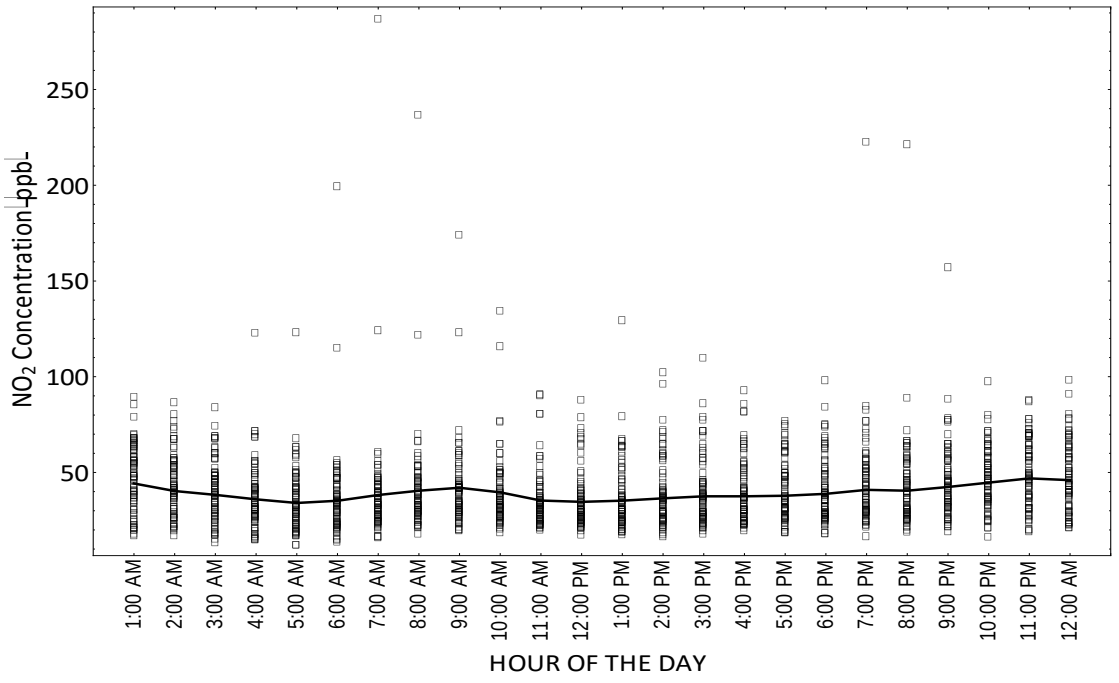

FIGURE 14 (B): HOURLY AVERAGE NO_2 CONCENTRATION FOR EACH DAY OF DATA ACQUISITION FROM MAY TO JULY

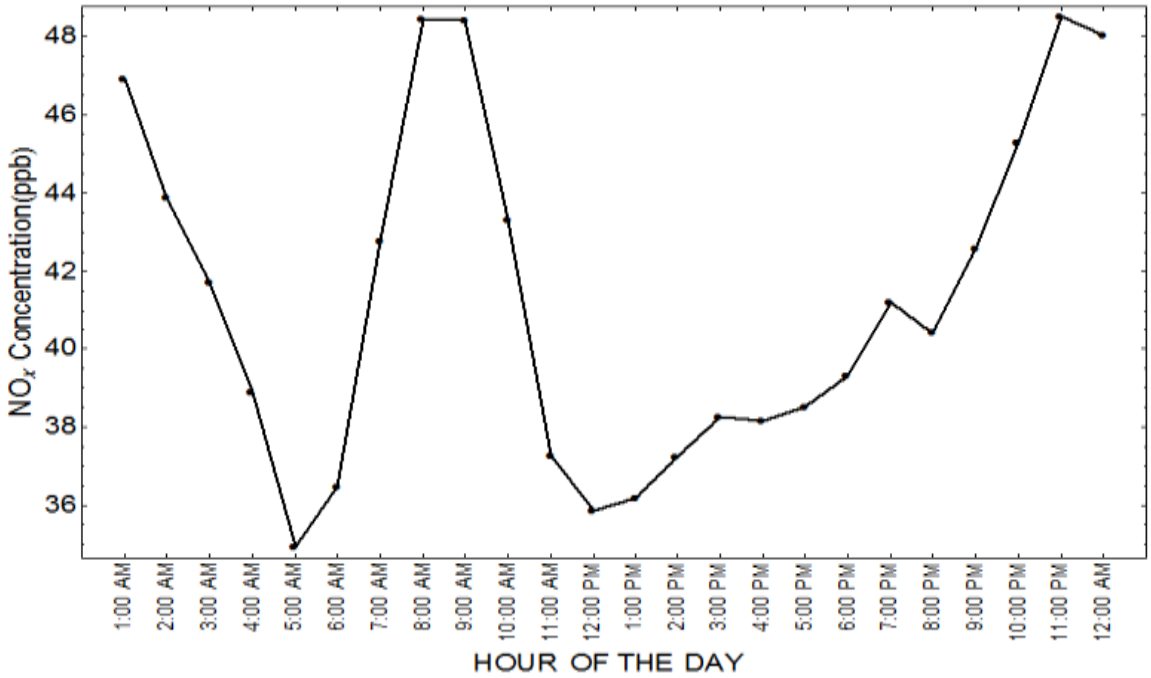

FIGURE 15 (A): DAILY HOURLY AVERAGE VARIATION OF NO_x IN AMBIENT AIR FROM MAY TO JULY

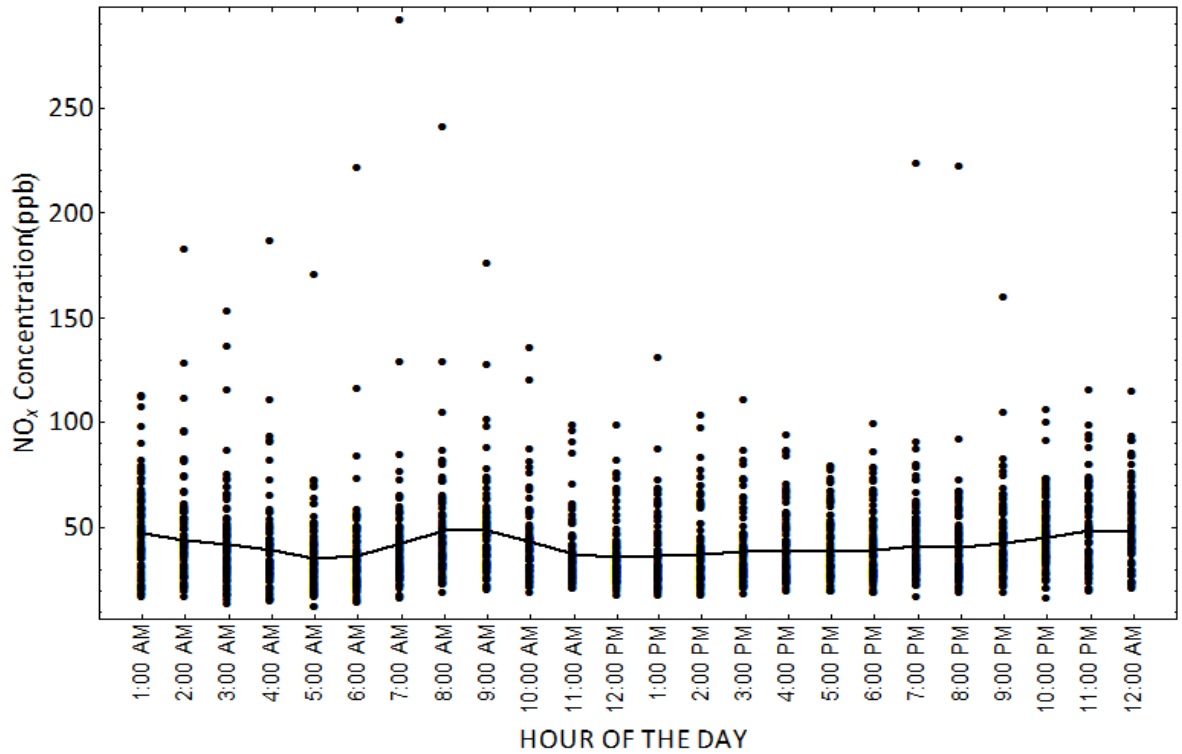

FIGURE 15 (B): HOURLY AVERAGE NO_x CONCENTRATION FOR EACH DAY OF DATA ACQUISITION FROM MAY TO JULY

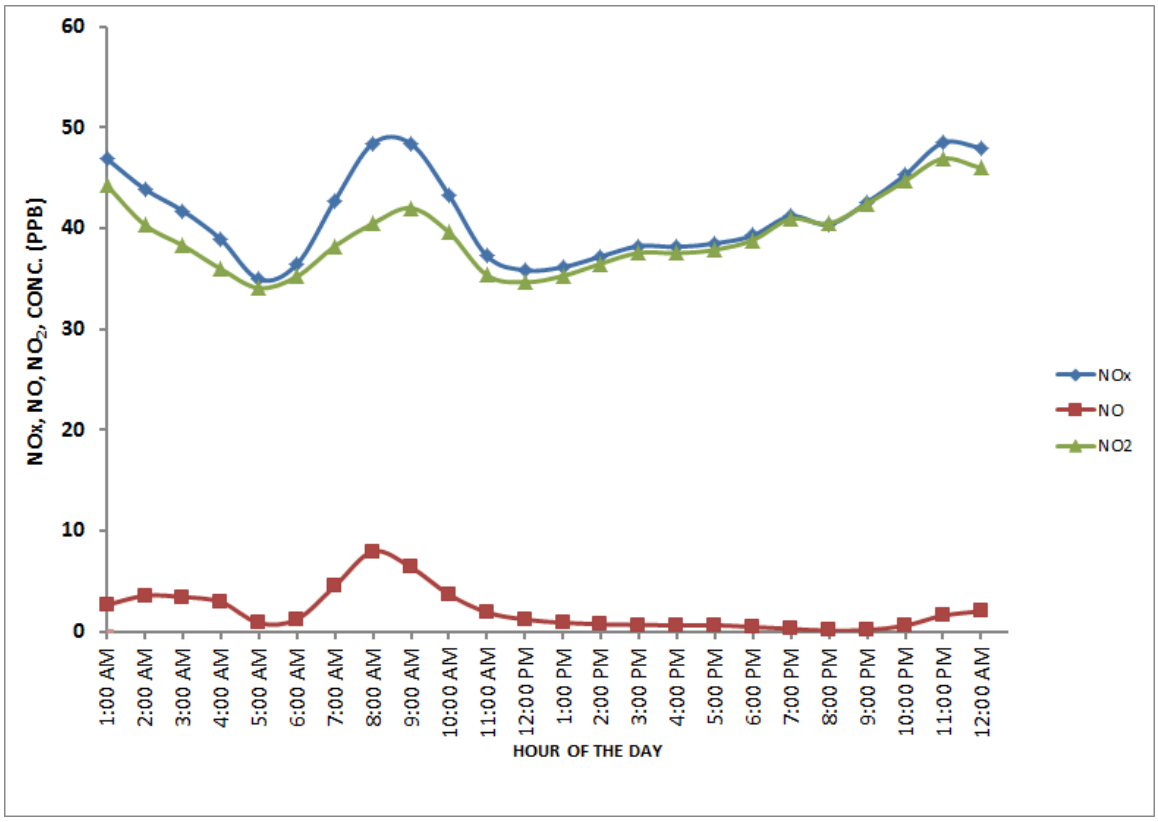

FIGURE 16: DAILY HOURLY AVERAGE VARIATION OF NO_x, NO_2 AND NO IN AMBIENT AIR FROM MAY TO JULY

4.3 Relationship between Hourly NOx, NO and NO_2 Concentrations and Meteorological Parameters (Temperature, Relative Humidity, Wind Speed and Air Pressure)

Visual comparison of NOx and meteorological parameters is carried out in figure 17. Going with the nature of the curves in figure 17, it is very difficult to vividly and visually ascertain the trend of these pollutants with meteorological parameters for atmospheric process is very intricate and complex. With that, the dimension of interactions among NOx and meteorological data may be absolutely evasive and beyond physical comparison as it is the case with figure 17.

In order to unravel this confusion and bring about consistent trends between daily hourly mean NOx concentration and meteorological parameters, stepwise regression analysis was employed to evaluate the correlation coefficients of daily hourly average of NO, NO_2 and NOx concentrations with the daily hourly average values of each of the meteorological parameters (temperature, humidity, wind speed). Through selection of statistically significant parameters influencing NOx concentrations, pressure and wind direction were disqualified. Pressure had a very infinitesimal variation during measurement period and wind direction is not a linear function, coupling it to form a linear relationship may be misleading, though it can be a perfect parameter when considering the non-linear relationship, which is beyond the scope and objectives of this research work. The result of the analysis produced by Minitab Statistical Software is presented in table 1.

NO, NO_2 and NOx were found to have positive correlation coefficients with one and another. NOx has statistically significant correlation coefficients of 0.578 and 0.889 with NO and NO_2 respectively with their p- value being less than 0.01. Similarly NO_2 also has

positive correlation coefficient of 0.141 ($p < 0.01$) with NO. This relationship is evidencing that these pollutants have common source and confirming the influence of traffic emission source.

Furthermore, the result shows that the positive correlation coefficients (0.162, 0.455, 0.449 respectively) of nitrogen oxides (NO, NO_2, NOx) with relative humidity were significant at the level of 0.05. In the night, when humidity has its maximum value, these pollutants maintained high concentrations because of the formation of nocturnal boundary layer (NBL) near the surface, which is stable thereby trapping these pollutants in the lower troposphere. This behavior is typical of urban areas being influenced by automobile source [35].

Table 1 also shows that nitrogen oxides have inverse correlation coefficients with wind speed in Dhahran city. This can be explained by the fact that a higher wind speed (except for very strong wind) improves the dispersion and mixing of these atmospheric pollutants emitted at closer sources (i.e, at highways and stationary sources), thereby minimizing the cumulative concentrations of these pollutants in the atmosphere. This behavior is in line with what was discovered in some other urban cities [12], [36].

Negative correlation coefficients (-0.319,-0.341,-0.419) exist between ambient air temperature and nitrogen oxides (NO_2, NO, NOx respectively) which are statistically significant ($p < 0.05$). The atmospheric temperature near the earth surface is intense during summer and this enhanced the vertical mixing and led to the increase of vertical mixing height. The continuous mixing of the atmospheric composition with the pollutants, resulting in minimizing the concentration of the nitrogen oxides in summer. This is also confirmed in some other cities as well [37].

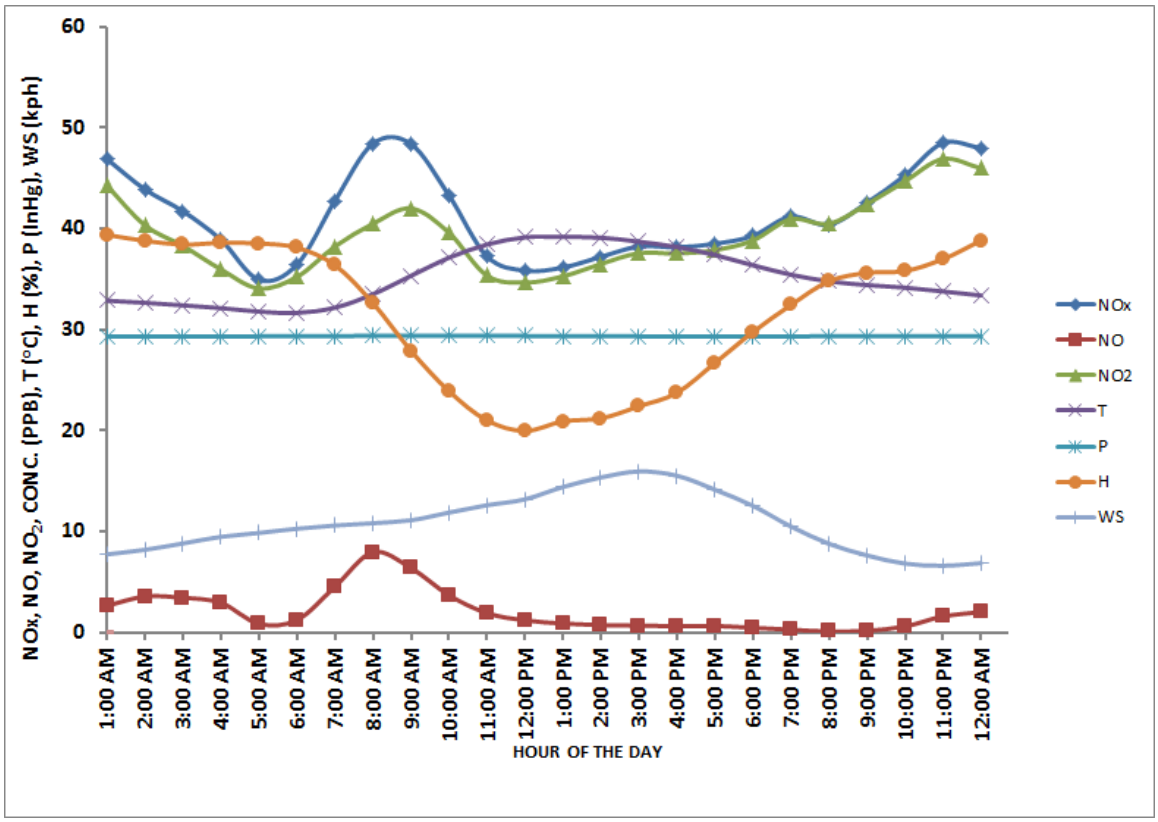

FIGURE 17: DAILY HOURLY VARIATION OF TEMPERATURE, HUMIDITY, WIND SPEED, PRESSURE, NO CONC., NO_2 CONC., AND NO_x CONC.

	NO2	NO	NOX	T	VW
NO	0.141	1			
P-VALUE	0.001				
NOX	0.889	0.578	1		
P-VALUE	0.000	0.003			
T	-0.319	-0.341	-0.410	1	
P-VALUE	0.019	0.003	0.041		
VW	-0.672	-0.154	-0.624	0.798	1
P-VALUE	0.000	0.013	0.001	0.000	
H	0.455	0.162	0.449	-0.963	-0.864
P-VALUE	0.005	0.051	0.028	0.000	0.000

TABLE 1: PEARSON CORRELATION COEFFICIENTS AND P-VALUES BETWEEN HOURLY MEAN NO, NO2 AND NOX CONCENTRATIONS AND METEOROLOGICAL PARAMETERS (AMBIENT TEMPERATURE, RELATIVE HUMIDITY, WIND VELOCITY)

4.4 Daily Average Concentrations of NO, NO_2 and NOx

Figure 18(a) is the plot of daily average concentration of NO_2, shown with it on the plot, the average measured concentration of NO_2 for all the three months (7^{th} May, 2015 – 30^{th} June 2015) and the maximum annual exposure limit as propounded by US EPA.

Figure 18(b) is the daily average temperature for each day of data acquisition with trendline to indication the average variation across all the data points.

Similarly, figure 19 also shows the plot of hourly average NO_2 concentration for each day of data acquisition, the daily hourly average of NO_2 concentration and maximum hourly exposure limit of 100 ppb, also according to US EPA. EPA regulates only nitrogen dioxide (NO_2) as a surrogate for this family of compounds (NOx) because it is the most prevalent form of NOx in the atmosphere that is generated by anthropogenic (human) activities. This explains the reason it is solely being shown on this plot. The NAAQS, agency established by EPA for the NO_2 and Ozone regulatory purpose, defines levels of air quality that are necessary, with a reasonable margin of safety, to protect public health (primary standard) and public welfare (secondary standard) from any known or suspected adverse effects of pollution. The primary and secondary standard for NO_2 is 53 parts per billion (ppb) (100 micrograms per cubic meter), annual arithmetic mean concentration and 100 ppb maximum limit for 1 hour exposure, as indicated in figures 18(a) and 19 respectively.

During the entire period of study, measured NO_2 concentrations had minimum concentration of 15.6 ppb on Saturday, 16^{th} May 2015; the day which marked the end of academic class in schools in Dhahran which as a result, students went in preparation for the finales. This reduced the influx of vehicles usually plying the highways; most

especially those usually visited the shopping malls around the KFUPM monitoring site. The maximum concentration of 94.7 ppb was also measured on Thursday, 16th July, 2015. This day also coincided with the "eidl day" that marked the end of Ramadan, which is usually celebrated with pump and pageantry. The large volume of vehicles on the highways in this day, probably due to visitation of nearby shopping malls, consequently resulted in high level of traffic emission.

Thirteen days out of 85 days in discussion were found to be above the maximum exposure limit of 53 ppb. The majority of days that exceeded the maximum allowed limit fell within week days and mostly in the months of May and June. The reason for this observation, asides for the openings of schools in Dhahran for academic activities which results in high traffic emission, could be linked to the temperature effect which aids photochemical cycles of NOx and ozone. According to equation (2.6) and (2.7), higher temperature favours more production of ozone, which may translate to reduction in NO_2 concentration in ambient air. This is observed in figures 18(a) and 18(b) where the change in temperature across the days correlated inversely with the NO_2 concentration (lower NO_2 concentration registered when temperature is high and vice versa). Higher concentration of NO2 was mostly measured for days whose average temperature falls below the average temperature for the whole measurement period and these days are essentially in the months of May and June. However, the average concentration of 41.19 ppb computed for the three months of study so far is still below this US EPA prescribed limit (53 ppb), though a bit higher than European standard of 40 ppb.

In the same vain, as seen from figure 19, hourly average NO_2 concentration happened to exceed the maximum hourly permissible limit of 100 ppb of both US EPA and European

standards for 18 days within the whole measurement period of three month (7^{th} May 2015 – 30^{th} June 2015).

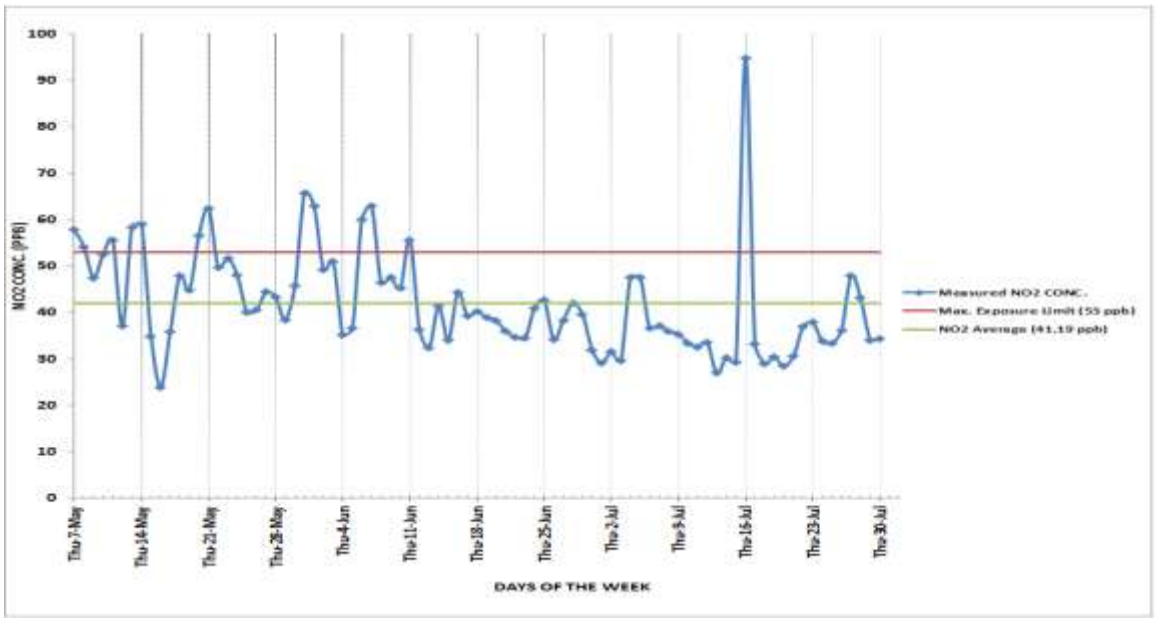

FIGURE 18 (A): DAILY AVERAGE OF NO_2 CONCENTRATION FOR MEASUREMENT FROM 7TH MAY, 2015 TO 30TH JULY 2015

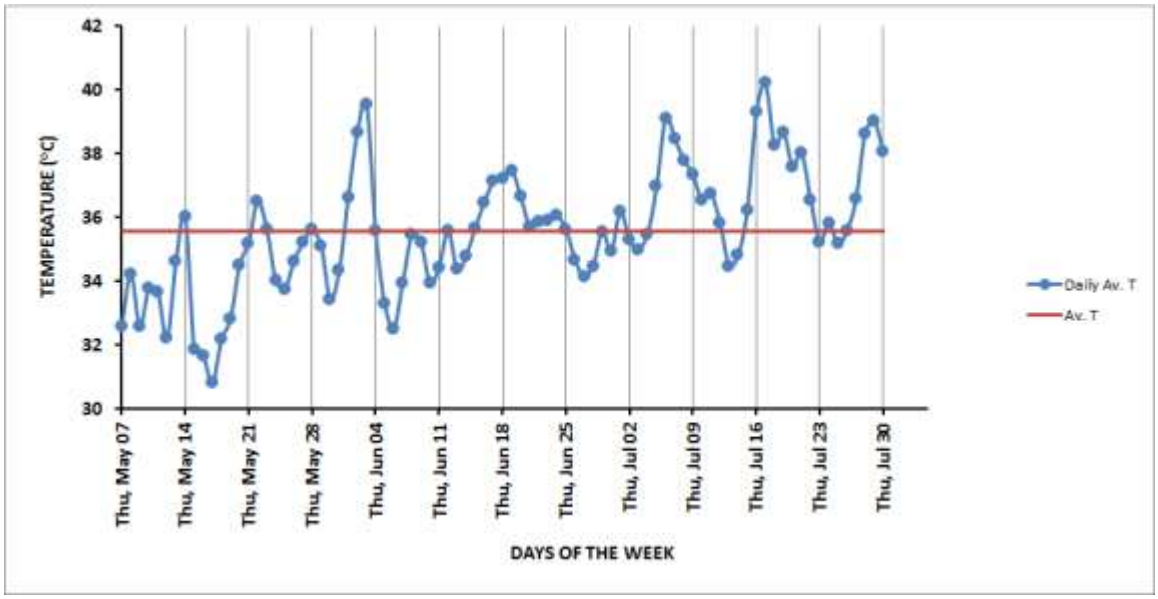

FIGURE 18 (B): DAILY AVERAGE VARIATION OF TEMPERATURE WITH THE OVERALL AVERAGE TEMPERATURE FOR MEASUREMENT FROM 7TH MAY, 2015 TO 30TH JULY 2015

.

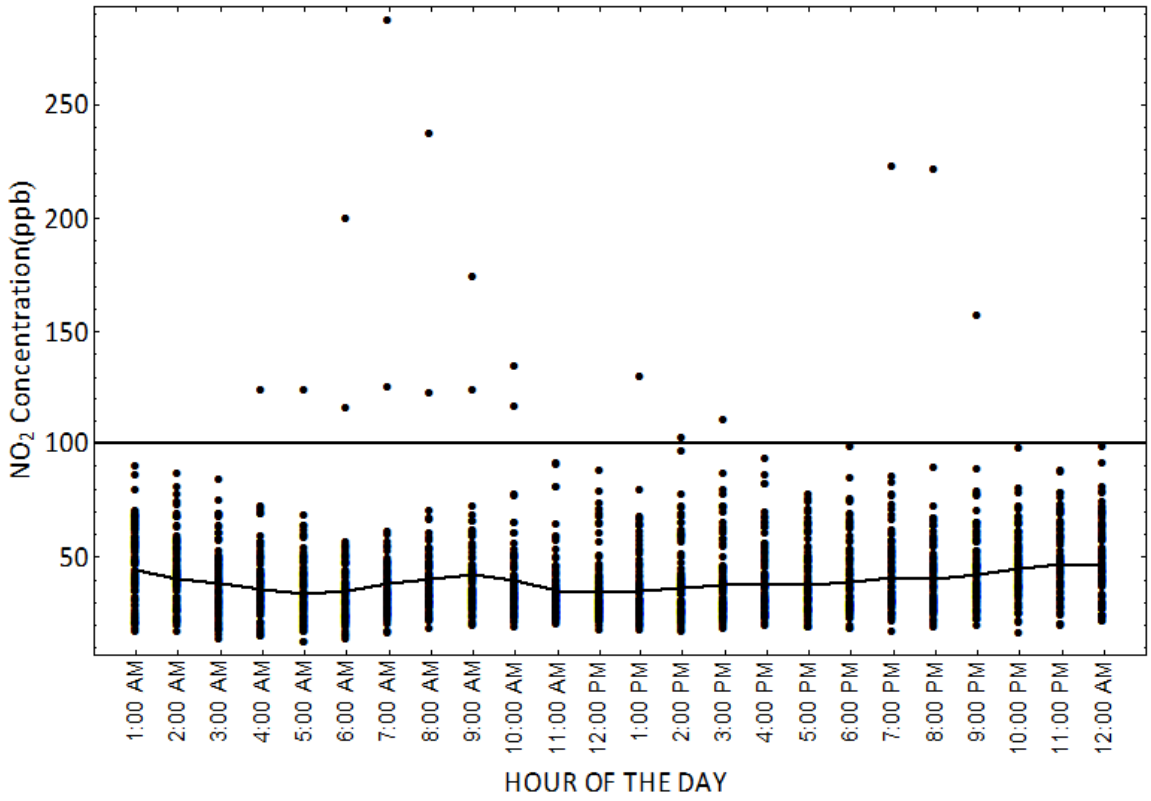

FIGURE 19: HOURLY AVERAGE OF NO_2 CONCENTRATION FOR EACH DAY OF DATA ACQUISITION FROM 7TH MAY, 2015 TO 30TH JULY 2015

4.5 Weekly Daily Average Concentration of NO, NO_2 and NO_X

Thursday is having higher concentration of NO_2 of almost 48.5 ppb, considering its weekly average as shown in figure 20, than any other day. It is followed by Sunday with approximately 44.3 ppb, Tuesday 39.2 ppb then Saturday 40.0 ppb. Monday and Wednesday are ties with approximately 41.8 ppb while Friday is least affected by NO_2 episode with approximate concentration of 37.7 ppb. Generally, weekends are least affected by traffic emissions, so it is expected that NO_2 concentration should drop just as observed in figures (18a) and (20). Weekdays NO_2 pollution episode takes the opposite situation.

The trend of NO in figure 20 shows the higher concentration during weekdays than weekends. Even though, Tuesday, a day within the week, has lower NO_2 concentration (39.2 ppb) than Saturday's (40 ppb) which is weekend, conversely, NO level on the former is higher than the latter. This entrenches the fact that the NO concentration is strongly attached to automobile source which is more vibrant on weekdays than weekends while NO_2 could be affected by many other sources either anthropogenic or biogenic asides automobile.

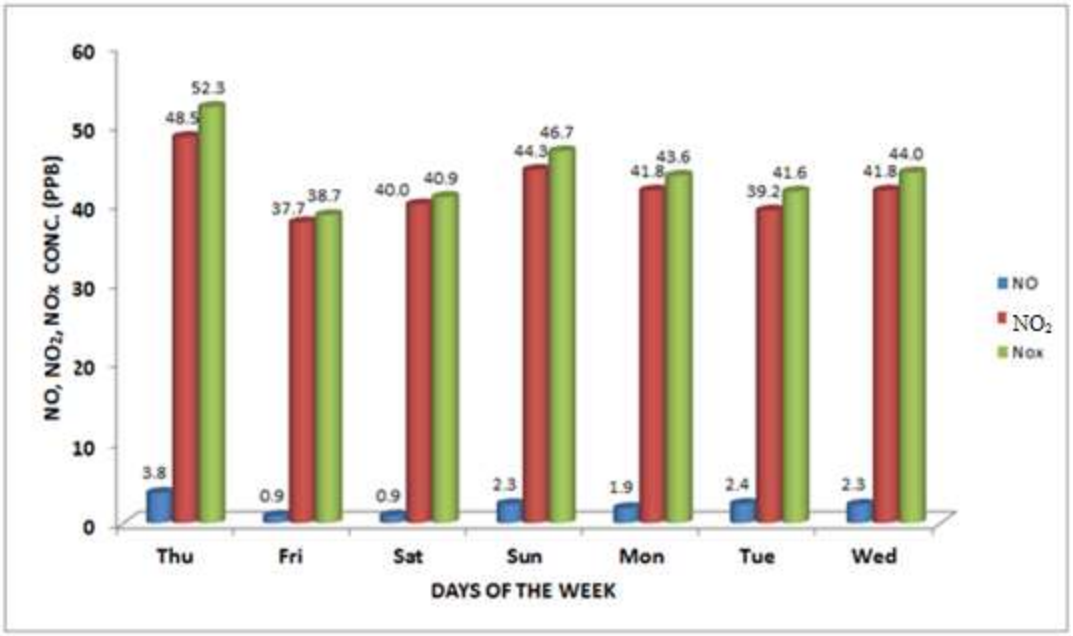

FIGURE 20: WEEKLY AVERAGE DAILY VARIATION OF NO_2 CONCENTRATION FOR MEASUREMENT FROM 7TH MAY, 2015 TO 30TH JULY 2015

4.6 Mathematical Model Result

Semi – empirical model equation 3.9 has been fitted to the daily average NOx pollution data and meteorological data of May and July 2015, summer season. The results of regression analysis performed with the Minitab software are given in table 2. Variables considered in the regression analysis are T (ambient air temperature), S (wind speed), H (relative humidity) and C_{j-1} (pollutant concentration of previous day).

When table 2 is examined, the R^2 value for the model is 0.54, with 60 data points. This R^2 value, which may not be as high as 0.9 and above (R^2 range for very good fit model), is an indication that some very important parameters were left out of the model. NOx episode is highly influenced by photochemical activities. The variables (solar radiation and ozone concentration) which would have represented this property (photochemical activities) in the model are not available as at the time of the study. However, R^2 value of 0.54 is a good indication that the model is valid, even without solar radiation and ozone concentration data.

Significant levels and standard error of each of the predictors are also shown in table 2. It was found out that all the variables are significant at the significant level of 0.01 (P- value < 0.01). This further proves the validity of the model.

The model, which was formulated, based on May and June data, is applied to July measurement of NOx concentration. Figure 21 shows the predicted and measured concentrations of NOx in the month of July clustered around the diagonal. The little variation between the diagonal line and some data points is probably due to the variation which cannot be explained by the model because of the incomplete predictors (solar radiation and ozone concentration) used in the model formulation. However, the

statistical analysis indicates the validity of the proposed model, even though some other vital variables are absent. Nevertheless the result so far is above the expectation and could serve as a platform for more inclusive and accurate model.

	REGRESSION COEF.	P-VALUE	SE COEF.
Ao	105.4	0.000	27.8
A1	1.267	0.006	0.679
A2	2.596	0.000	0.536
A3	-0.368	0.007	0.132
A4	0.288	0.003	0.0948
R^2	0.54		

TABLE 2: THE RESULT OF STEPWISE REGRESSION ANALYSIS FOR NO_x CONCENTRATION ACQUIRED IN MAY AND JUNE, 2015

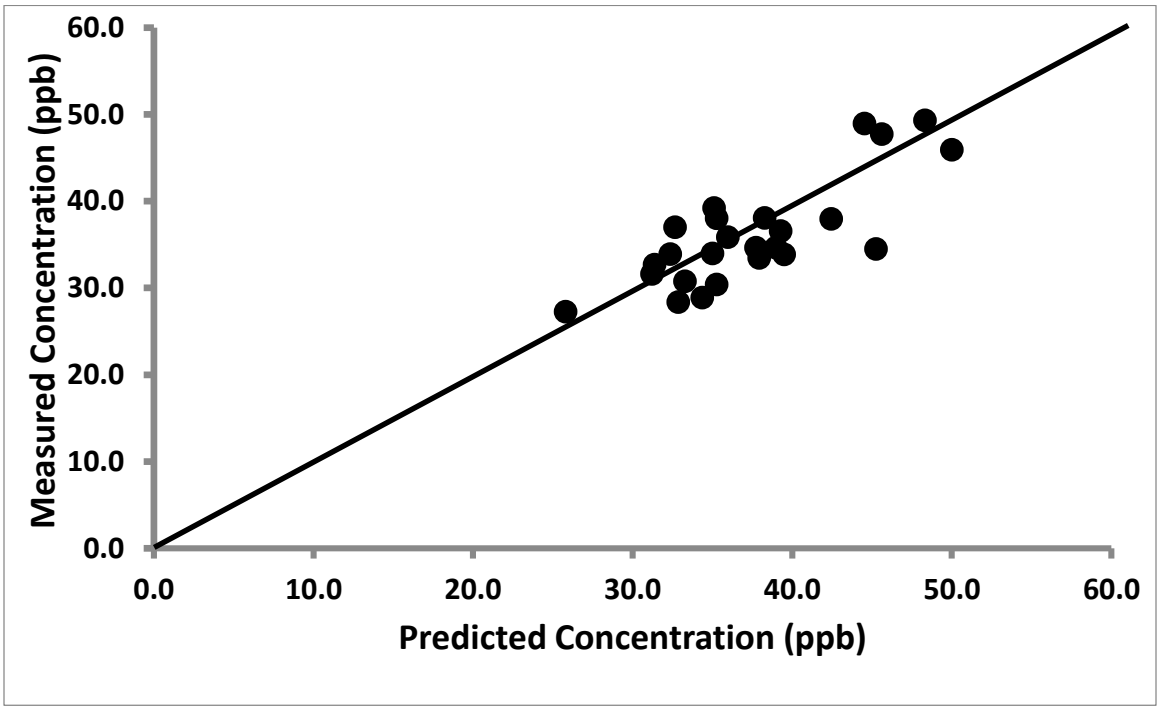

FIGURE 21: PLOT OF MEASURED AND MODELED NO_x CONCENTRATION FOR THE MONTH OF JULY.

CHAPTER 5

5.0 CONCLUSIONS

The measurement of NO, NO_2, NOx and meteorological data (ambient air temperature, ambient air pressure, relative humidity, wind speed and wind direction) were carried out in the city of Dhahran between May 7th, 2015 and July 30th, 2015. The analysis of the acquired data was carried out with Mathematica program, MiniTab and Microsoft Excel software package. Daily hourly average, daily mean and weekly daily average concentrations of the NOx pollutants and meteorological data were computed, which were used for the analysis. Both visual and statistical analysis (regression analysis) was employed to establish the relationship between the pollutant concentrations and weather data. Finally a semi empirical model was formulated to reveal the relation between NOx pollutants and weather data and also predict the pollutant data given weather conditions.

During the measurement period which took place for 85 days, 13 days exceeded the maximum allowable exposure limit of 53 ppb annual mean concentration of NO_2 in the ambient air. However, the average concentration of the whole measured data is still below this limit. More so, the hourly limit of 100 ppb set by EPA and European standard was also exceeded for 18 days within the data acquisition period.

The daily hourly average variation of NO, NO_2, and NOx showed that the urban atmosphere of this city is strongly affected by motor traffic and photochemistry as the maximum NOx concentrations were measured in weekdays while minimum NOx concentrations were recorded in weekends . The concentrations of these pollutants were found to be linked with one another and indirectly affected by meteorological conditions. Regression analysis of the daily hourly NOx concentrations of the measured data

glaringly established that ambient air temperature and wind speed have negative correlation coefficient with the NOx concentrations (NO + NO_2), whereas relative humidity was found to have positive correlation coefficient.

Lastly, the semi empirical model (using simple box model) formulated, established a linear relationship between NOx daily average concentrations in the ambient air and meteorological data (temperature, wind speed and relative humidity). It further revealed that the previous day concentration is a deterministic factor for NOx concentrations measured in the ambient air. The model performed well to the expectation with R^2 of 0.54, though it is still subject to modification and improvement.

APPENDIX A

Data Sample

Example of raw data acquired on the 10th of May, 2015 between 5 AM and 6 AM.

Time	NO Conc.	NOx Conc.	NO_2 Conc	Status	T	RH	P	WD	WS
16389,	0.000025,	0.027780,	0.027755,	8202,	,	,	,	221,	5.2
16390,	0.000024,	0.027782,	0.027757,	8202,	,	,	,	218,	5.2
16391,	0.000024,	0.027782,	0.027758,	8202,	,	,	,	217,	5.3
16392,	0.000023,	0.027782,	0.027759,	8202,	,	,	,	216,	5.4
16393,	0.000022,	0.027782,	0.027760,	8202,	,	,	,	216,	5.4
16394,	0.000021,	0.027782,	0.027761,	8202,	,	,	,	217,	5.7
16395,	0.000020,	0.027782,	0.027761,	8202,	,	,	,	218,	5.9
16396,	0.000019,	0.027782,	0.027762,	8202,	,	,	,	221,	6.1
16397,	0.000018,	0.027781,	0.027763,	8202,	,	,	,	222,	5.9
16398,	0.000018,	0.027781,	0.027764,	8202,	,	,	,	223,	5.8
16399,	0.000017,	0.027781,	0.027765,	8202,	,	,	,	220,	5.8
16400,	0.000016,	0.027781,	0.027765,	8202,	,	,	,	217,	6.1
16401,	0.000015,	0.027781,	0.027766,	8202,	86.0,	33.4,	29.37,	,	
16401,	0.000015,	0.027781,	0.027766,	8202,	,	,	,	212,	6.2
16402,	0.000014,	0.027781,	0.027767,	8202,	,	,	,	212,	5.7
16403,	0.000014,	0.027783,	0.027769,	8202,	,	,	,	213,	5
16404,	0.000013,	0.027784,	0.027771,	8202,	,	,	,	218,	4.6
16405,	0.000013,	0.027786,	0.027773,	8202,	,	,	,	220,	4.2
16406,	0.000013,	0.027787,	0.027774,	8202,	,	,	,	207,	3.4
16407,	0.000012,	0.027789,	0.027776,	8202,	,	,	,	203,	2.9
16408,	0.000012,	0.027790,	0.027778,	8202,	,	,	,	206,	3.2
16409,	0.000012,	0.027791,	0.027780,	8202,	,	,	,	224,	3.9
16410,	0.000011,	0.027793,	0.027782,	8202,	,	,	,	227,	4.2
16411,	0.000011,	0.027794,	0.027783,	8202,	,	,	,	224,	4.2
16412,	0.000011,	0.027796,	0.027785,	8202,	,	,	,	218,	4
16413,	0.000010,	0.027797,	0.027787,	8202,	,	,	,	218,	4
16414,	0.000010,	0.027799,	0.027789,	8202,	,	,	,	218,	3.9
16415,	0.000009,	0.027799,	0.027790,	8202,	,	,	,	226,	3.9
16416,	0.000009,	0.027800,	0.027791,	8202,	86.0,	33.5,	29.37,	,	
16417,	0.000009,	0.027800,	0.027791,	8202,	,	,	,	232,	4.3
16417,	0.000008,	0.027800,	0.027792,	8202,	,	,	,	233,	4.6
16418,	0.000007,	0.027800,	0.027793,	8202,	,	,	,	229,	5
16419,	0.000007,	0.027801,	0.027794,	8202,	,	,	,	223,	4.6
16420,	0.000006,	0.027801,	0.027795,	8202,	,	,	,	222,	4.6
16421,	0.000005,	0.027802,	0.027796,	8202,	,	,	,	222,	4.6

APPENDIX B

Mathematica Code

(1) This code below read in a month data from the computer hard disk into the RAM for the access to Mathematica program.

```
monthData = {}; For[i = 1, i ≤ 30, i++, st = OpenRead["2015 − month − " <
> ToString[i] <> ". txt"];  Read[st, Record]; Read[st, Record]; st
= ToExpression[ReadList[st, {Record, Record, Record, Record, Record, Record, Record,
                Record, Record, Record},
        {RecordSeparators → {", ", "\n"}}]]; Close[st]; no1xF = lst[[All, 3]]; no1x
                = DeleteCases[no1xF, Null]; AppendTo[mayData, no1x]];
```

(2) To add up all data for every month, the code below is used

```
addata = Join[monthData1, monthData2, monthData3, etc];
```

(3) To partition into the hourly measured data for the purpose of computing hourly or daily or weekly average variation, the code below is employed

```
noTparfile = {}; For[n = 1, n ≤ Length[addata], n++, w
                = Partition[addata[[n]], k]; AppendTo[noTparfile, w]];
```

(4) To collect from each of the month, data acquired with same hour of the day, the code below is employed

```
noPhrsort = Table[noxPparfile[[i, j]], {j, 1,24}, {i, 1,75}];
noPfilemap = Flatten/@noPhrsort;
```

(5) To compute hourly or daily or weekly average from sorted data, the following code is used;

```
hourlyavernoP = Mean/@noPfilemap
```

(6) To compute standard deviation, we used;

```
std = StandardDeviation/@noPfilemap
```

APPENDIX C

LabView Code

(1) This LabView code calls the SUBVI of weather station and NOx analyser and attached to their data set, the time stamp.

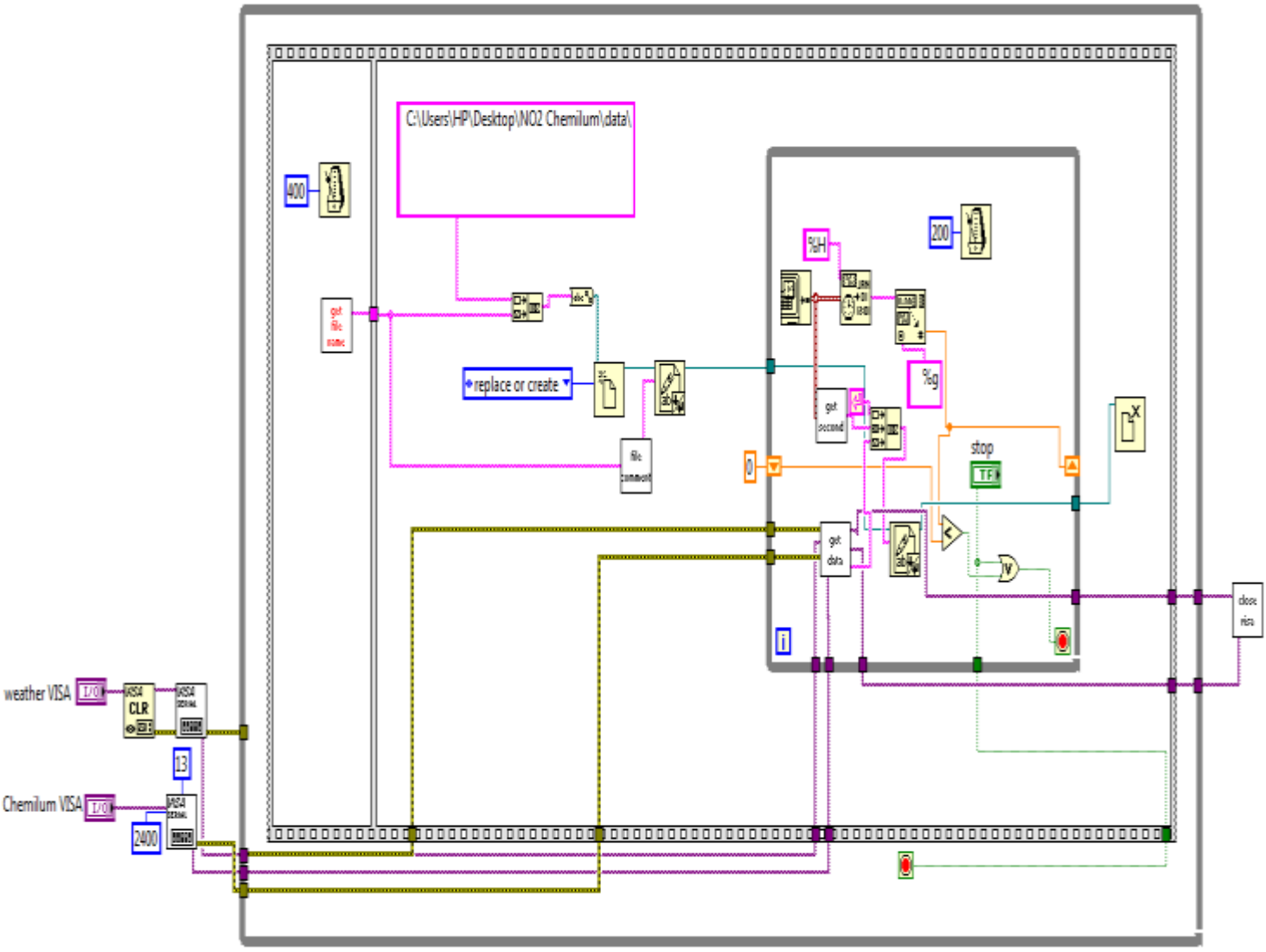

(2) This SUBVI synchronizes both weather station and NOx-analyser for simultaneous data logging.

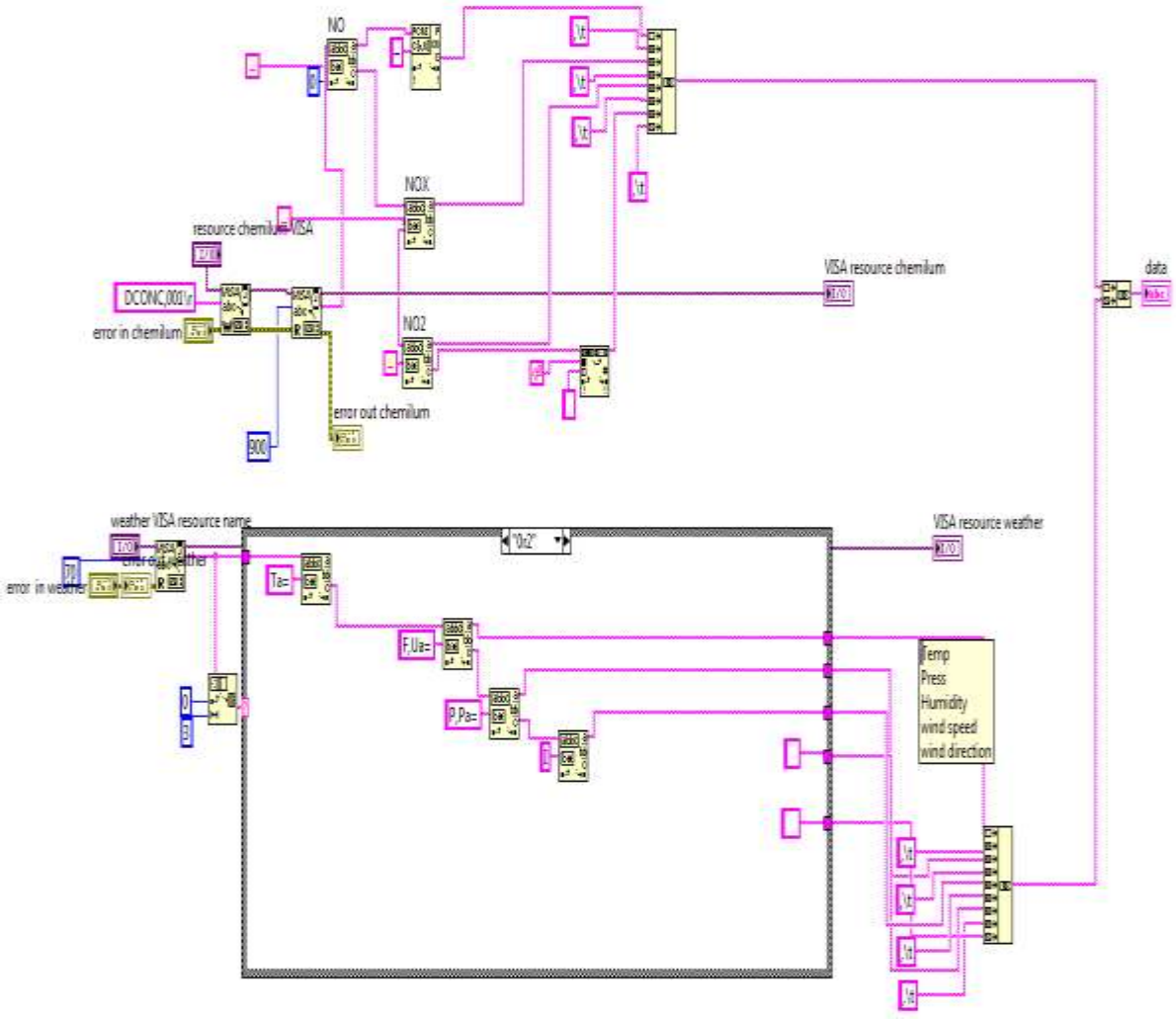

REFERENCES

[1] Z. X. Han, Suqin, Bian Hai, Feng Yinchang, Liu Aixia, Li Xiangjin, Zeng Fang, "Analysis of the Relationship between O3, NO and NO2 in Tianjin, China," *Aerosol Air Qual. Res.*, no. 2, pp. 128–139, 2011.

[2] X. Wang and D. L. Mauzerall, "Evaluating impacts of air pollution in China on public health: Implications for future air pollution and energy policies," *Atmos. Environ.*, vol. 40, no. 9, pp. 1706–1721, 2006.

[3] A. Richter, J. P. Burrows, H. Nüss, C. Granier, and U. Niemeier, "Increase in tropospheric nitrogen dioxide over China observed from space.," *Nature*, vol. 437, no. 7055, pp. 129–32, Sep. 2005.

[4] H. Akinmoto, "Global Air Quality and Pollution," *Sci. 302*, pp. 1716–1719, 2003.

[5] I. A. Hassan, J. M. Basahi, I. M. Ismail, and T. M. Habeebullah, "Spatial Distribution and Temporal Variation in Ambient Ozone and Its Associated NOx in the Atmosphere of Jeddah City, Saudi Arabia," *Aerosol Air Qual. Res.*, pp. 1712–1722, 2013.

[6] M. Kampa and E. Castanas, "Human health effects of air pollution.," *Environ. Pollut.*, vol. 151, no. 2, pp. 362–7, 2008.

[7] K. Al-Ahmadi and A. Al-Zahrani, "Spatial autocorrelation of cancer incidence in Saudi Arabia.," *Int. J. Environ. Res. Public Health*, vol. 10, no. 12, pp. 7207–28, 2013.

[8] National Research Council of the National Academies, *Emergency and continuous exposure guidance levels for selected submarine contaminants. Volume 1*. 2007.

[9] M. Z. Jacobson, *Fundamental of Atmospheric Modeling*, vol. 53. 1989.

[10] Y. Itano, M. Yamagami, and T. Ohara, "Estimation of Primary NO 2 / NOx Emission Ratio from Road Vehicles Using Ambient Monitoring Data," *Stud. Atmos. Sci.*, vol. 1, no. 2, pp. 1–7, 2014.

[11] R. Kurtenbach, J. Kleffmann, A. Niedojadlo, and P. Wiesen, “Primary NO2 emissions and their impact on air quality in traffic environments in Germany,” *Environ. Sci. Eur.*, vol. 24, no. 1, p. 21, Jun. 2012.

[12] D. M. Agudelo-Castaneda, E. C. Teixeira, and F. N. Pereira, “Time- Series analysis of surface ozone and nitrogen oxides concentration in an urban area at Brazil,” *Atmos. Pollut. Res.*, vol. 5, pp. 411–420, 2014.

[13] D. C. Carslaw, “Evidence of an increasing NO2/NOX emissions ratio from road traffic emissions,” *Atmos. Environ.*, vol. 39, no. 26, pp. 4793–4802, 2005.

[14] P. B. Julian E. Andrews, “An Introduction to Environmental Chemistry, 2nd Edition -.” [Online]. Available: http://eu.wiley.com/WileyCDA/WileyTitle/productCd-0632059052.html. [Accessed: 05-Mar-2016].

[15] B. de Foy, J. R. Vareala, L. T. Molina, and M. J. Molina, “Rapid ventilation of the Mexico City basin and regional fate of the urban plume,” *Atmos. Chem. Phys.*, vol. 6, no. 2000, pp. 2321–2335, 2006.

[16] A. O. Langford, C. J. Senff, R. J. Alvarez, R. M. Banta, and R. M. Hardesty, “Long-range transport of ozone from the Los Angeles Basin: A case study,” *Geophys. Res. Lett.*, vol. 37, no. 6, p. n/a–n/a, 2010.

[17] X. Lan, R. Talbot, P. Laine, B. Lefer, J. Flynn, and A. Torres, “Seasonal and Diurnal Variations of Total Gaseous Mercury in Urban Houston, TX, USA,” *Atmosphere (Basel).*, vol. 5, no. 2, pp. 399–419, 2014.

[18] V. R. Kotamarthi, P. V Doskey, S. R. Springston, P. Hyde, and J. S. Ga, “Modeling of trace gases from the 1998 North Central Mexico forest fire smoke plume , as measured over Phoenix,” pp. 3227–3264, 2006.

[19] "Environmental Protection Agency, Primary National Ambient Air Quality Standards for Nitrogen Dioxide; Final Rule, Federal Register / Vol. 75, No. 26 / Tuesday, February 9, 2010 / Rules and Regulations." [Online]. Available: https://www.federalregister.gov/articles/2015/10/26/2015-26594/national-ambient-air-quality-standards-for-ozone. [Accessed: 05-Mar-2016].

[20] "Nitrogen oxides (NOx) emissions - European Environmental Agency."

[21] J. H. Seinfeld and S. N. Pandis, *ATMOSPHERIC From Air Pollution to Climate Change SECOND EDITION*. 2006.

[22] N. Hatzianastassiou, C. Matsoukas, a. Fotiadi, K. G. Pavlakis, E. Drakakis, D. Hatzidimitriou, and I. Vardavas, "Global distribution of Earth's surface shortwave radiation budget," *Atmos. Chem. Phys. Discuss.*, vol. 5, no. 4, pp. 4545–4597, 2005.

[23] "Tropospheric Ozone and Nitrogen Oxides." [Online]. Available: https://faculty.washington.edu/jaegle/558/ozone_NOx.pdf.

[24] I. Barnes and K. J. Rudziński, "Disposal of Dangerous Chemicals in Urban Areas and Mega Cities: Role of Oxides and Acids of Nitrogen in Atmospheric Chemistry," *NATO Sci. Peace Secur. Ser. C Environ. Secur.*, vol. 120, no. 2, pp. 15–29, 2013.

[25] G. Villena, I. Bejan, R. Kurtenbach, P. Wiesen, and J. Kleffmann, "Development of a new Long Path Absorption Photometer (LOPAP) instrument for the sensitive detection of NO_2 in the atmosphere," *Atmos. Meas. Tech.*, vol. 4, no. 8, pp. 1663–1676, Aug. 2011.

[26] "Chemiluminescence NO, NO2, NOx Monitor." [Online]. Available: http://www.k2bw.com/chemiluminescence.htm. [Accessed: 27-Apr-2016].

[27] "EC9841 Oxides of Nitrogen Analyzer, User Manual from Ecotech Environmental Monitoring Solution."

[28] "Orion 420 Weather Station Manual from Columbia Weather System." .

[29] “Dhahran - Google Maps.” [Online]. Available: https://www.google.com.sa/maps/place/Dhahran/@26.2280149,49.9032827,11z/data=!3m1!4b1!4m2!3m1!1s0x3e49e6db1c9b42e3:0x4df99b838777731. [Accessed: 27-Apr-2016].

[30] N. Topqu, B. Keskinler, M. Bayramo, and M. Akqay, “AIR POLLUTION M O D E L L I N G IN E R Z U R U M CITY,” vol. 79, no. August 1991, pp. 9–13, 1993.

[31] A. Karppinen, J. Kukkonen, T. Elolähde, M. Konttinen, and T. Koskentalo, “A modelling system for predicting urban air pollution:,” *Atmos. Environ.*, vol. 34, no. 22, pp. 3735–3743, 2000.

[32] Z. Zlatev, *Computer Treatment of Large Air Pollution Models*. Springer Science & Business Media, 2012.

[33] J. A. Adame, A. Lozano, J. P. Bolívar, B. A. De la Morena, J. Contreras, and F. Godoy, “Behavior, distribution and variability of surface ozone at an arid region in the south of Iberian Peninsula (Seville, Spain).,” *Chemosphere*, vol. 70, no. 5, pp. 841–9, Jan. 2008.

[34] K. Park, J. Y. Park, J. H. Kwak, G. N. Cho, and J. S. Kim, “Seasonal and diurnal variations of ultrafine particle concentration in urban Gwangju, Korea: Observation of ultrafine particle events,” *Atmos. Environ.*, vol. 42, no. 4, pp. 788–799, 2008.

[35] G. B. Raga, D. Baumgardner, T. Castro, A. Mart??nez-Arroyo, and R. Navarro-Gonz??lez, “Mexico City air quality: A qualitative review of gas and aerosol measurements (1960-2000),” *Atmos. Environ.*, vol. 35, no. 23, pp. 4041–4058, 2001.

[36] A. M. Jones, R. M. Harrison, and J. Baker, “The wind speed dependence of the concentrations of airborne particulate matter and NOx,” *Atmos. Environ.*, vol. 44, no. 13, pp. 1682–1690, Apr. 2010.

[37] R. Jayamurugan, B. Kumaravel, S. Palanivelraja, and M. P. Chockalingam, “Influence of Temperature, Relative Humidity and Seasonal Variability on Ambient Air Quality in a Coastal Urban Area,” *Int. J. Atmos. Sci.*, vol. 2013, pp. 1–7, 2013.

VITAE

Name	:	Mumin Abdulahi
Nationality	:	Nigerian
Date of Birth	:	September 10, 1985
Email	:	mumentum2@gmail.com
Address	:	27, Ibilade Street, Iyana church, Iwo Road, Ibadan, Oyo State, 23402, Nigeria
Academic Background	:	BSc. in Engineering Physics, Obafemi Awolowo University, Ile-Ife, Osun State, Nigeria